CHAPTER

Techniques for studying mechanobiology

1

Eimear B. Dolan[*,†,‡], **Stefaan W. Verbruggen**[§,¶], **Rebecca A. Rolfe**[||]

School of Pharmacy, Royal College of Surgeons in Ireland, Dublin, Ireland[*] *Discipline of Anatomy, School of Medicine, College of Medicine Nursing and Health Sciences, National University of Ireland, Galway, Ireland*[†] *Institute for Medical Engineering Science, Massachusetts Institute of Technology, Cambridge, MA, United States*[‡] *Department of Biomedical Engineering, Columbia University, New York, NY, United States*[§] *Institute of Bioengineering, School of Engineering and Materials Science, Queen Mary University of London, London, United Kingdom*[¶] *Department of Zoology, School of Natural Sciences, Trinity College Dublin, Dublin, Ireland*[||]

ABBREVIATIONS

2D	two-dimensional
3D	three-dimensional
AFM	atomic force microscopy
Ca^{2+}	calcium ion
cDNA	complementary DNA
CFD	computational fluid dynamics
CRISPR	clustered regularly interspaced short palindromic repeats
DIC	digital image correlation
ELISA	enzyme-linked immunosorbent assay
ECM	extracellular matrix
FE	finite element
FP	fluorescent protein
FRAP	fluorescent recovery after photobleaching
FRET	fluorescent resonance energy transfer
FSI	fluid-solid interaction
GPCR	G-protein-coupled receptor
IHC	immunohistochemistry
mRNA	messenger RNA
PIV	particle image velocimetry
qRT-PCR	quantitative real-time polymerase chain reaction
TFM	traction force microscopy

Mechanobiology in Health and Disease. https://doi.org/10.1016/B978-0-12-812952-4.00001-5
© 2018 Elsevier Ltd. All rights reserved.

1 INTRODUCTION TO MECHANOBIOLOGY

Mechanobiology is a field at the forefront of biomedical investigation, situated at the interface between the fields of engineering and biology. While new examples of the human body adapting or responding to mechanical loading are regularly being discovered, this phenomenon has long been observed in multiple tissue types and across numerous anatomical locations. Examples of tissue adaptation in response to changes in loading include bone, cartilage, tendon, vessels, heart, lung, and skin [1–7]. Each of these cases involves cell-driven responses by tissues and organs to loading, requiring translation of loading that occurs at the whole-organ scale down to mechanical stimulation of individual cells. The resulting changes in cell activity are then manifested back up through the scales, causing adaption at the tissue or organ level [8].

While intricately related to what could be termed "classical" biomechanics, mechanobiology can be thought of as its mirror opposite. Biomechanics largely concerns the study of the physical effects and interactions induced by biological activity (e.g., the forces imparted onto the ground during running), whereas mechanobiology describes the biological response to an applied mechanical stimulus (e.g., the loss of the bone in low-gravity environments). Therefore, while mechanobiological effects can be observed at the scale of an organ or organism, they are fundamentally the result of changes wrought by cells in response to mechanical stimuli [9]. In fact, it has been shown that most eukaryotic cells themselves exert force on their surrounding tissues, even in the absence of any external mechanical stimulus [10,11]. Furthermore, it has been proposed that all cells are mechanosensitive [12], as forces are essential for basic cellular functions like mitosis and migration [13,14]. Thus, mechanobiology is fundamentally a multiscale phenomenon, spanning the length scales from the very smallest molecules to whole organs and presenting unique challenges to researchers attempting to further our understanding. This complex relationship across multiple scales is illustrated in Fig. 1.

The objective of this chapter is to introduce researchers from various backgrounds to some of the wide range of experimental and computational techniques being applied to advance the study of mechanobiology. The first section examines investigative methods at the organ and tissue level, including animal models and tissue-engineering techniques. The second section moves toward the cell and molecular levels, introducing imaging methods, biochemical assays, and molecular analysis techniques to determine the biological responses to mechanical stimuli. The final section describes computational methods, which have been applied at multiple scales to analyze imaging data, quantify loading experienced by biological tissues, and predict structural responses to mechanical stimuli.

Mechanical stimulation is transferred down from organ to molecular scales, with various animal models (e.g., the rat ulnar loading model [15]), tissue-engineering bioreactors (e.g., spinner-flask bioreactor [16]), cell culture techniques (e.g., stretching individual cells [17]), and cytoskeletal disruption [18] used to

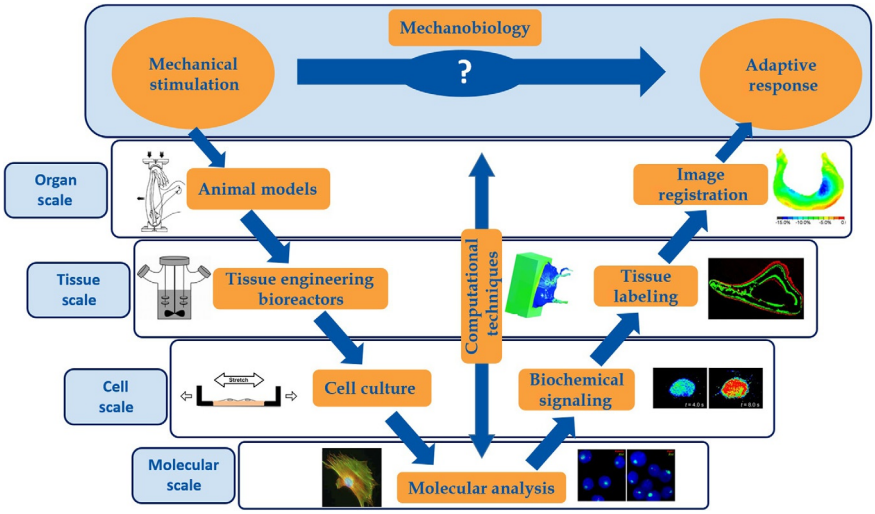

FIG. 1

Mechanobiology describes the adaptation of the body to mechanical stimulation and occurs across multiple scales, with researchers using a range of techniques to apply loading and measure the response at different scales.

replicate this experimentally. These stimuli are then transduced into biochemical and structural responses, with a range of techniques such as RNA assays (e.g., in situ hybridization on RNA analysis of gene expression [19]), biochemical assays (e.g., calcium signaling [20]), tissue labeling (e.g., tetracycline-alizarin staining for bone tissue growth [21]), and imaging techniques (e.g., image registration of knee menisci [22]) applied to measure these. Computational techniques (such as FSI modeling [23]) can operate across multiple levels, acting as a bridge across the length scales to model in vivo mechanobiology.

2 ANIMAL MODELS AND TISSUE ENGINEERING TO STUDY MECHANOBIOLOGY

2.1 ANALYSIS OF A SINGLE CELL

Single-cell investigations are advantageous for understanding cell behavior in response to specific stimuli (mechanotransduction). The results of single-cell investigations can be used to guide the development of mechanical environments that elicit favorable cell responses and inform tissue-engineering approaches [24,25]. Single-cell investigations are also used to investigate cell material properties, vital information that is required for computational investigations [26]. Force-application techniques are used to investigate single-cell mechanics, whereby the cell is

deformed in some way by a known force or stress and its mechanical and/or biochemical response is measured. Typically, the surface of the cell is indented or extended [26,27]. There are a number of force-application techniques available, as discussed in detail by Rodriguez et al. [26] and summarised in Fig. 2. Optical tweezers, atomic force microscopy (AFM), and micropipette aspiration are commonly used tools for single-cell investigation, shown in Fig. 2.

2.1.1 Force application techniques to analyze a single cell

2.1.1.1 Optical tweezers

Optical tweezers (often referred to as optical trap) are one method often used to apply a known force to a cell. This technique was developed by Arthur Ashkin in 1970 [28] and was originally used to trap individual atoms, viruses, and bacteria [29]. In this method, nano- to micron-sized beads are attached to the cell membrane. Displacement of the cell membrane is controlled by directing infrared lasers at the transparent beads. When photons pass through the beads, there is a change in their direction. The change in direction causes a change in momentum, resulting in a force on the bead. This change is dependent on the refractive index of the beads. Optical tweezers can exert forces in excess of 100 pN on particles ranging in size from nanometers to microns while simultaneously measuring the 3D displacement of the trapped particle with subnanometer accuracy and submillisecond time resolution [30].

2.1.1.2 Atomic force microscopy

AFM was first developed to probe nanoscale features of solid materials using its high sensitivity to intermolecular forces ($\sim$pN) and spatial resolution ($\sim$nm). More recently, AFM has been used throughout the literature to measure the apparent elasticity of living cells. An AFM system generally consists of a probing tip attached to a flexible cantilever that is lowered onto the cell, and the deflection of the cantilever is monitored. The local Young's modulus (E) of a living cell can be measured by recording the force acting on the AFM tip while it is indented into a cell, which results in a force-displacement curve. This force-displacement curve can be used to calculate the force-indentation curve by fitting it with the Hertz model (contact mechanics) allowing the estimation of the local E; a detailed description is provided in [31,32]. The following two conditions must be met for an accurate measurement: (a) The indentation depth is not more than $\sim$10% of the sample thickness [33,34], and (b) the indentation depth is $>$200 nm [35]. Additionally, the variable shape of a typical AFM probe will determine the nature of the force-deformation curve [27]. AFM indentation is typically performed on highly localized regions of the cell, probing individual structures and determining the heterogeneity of cell.

2.1.1.3 Micropipette aspiration

A micropipette is a small glass capillary with an internal diameter smaller than that of a cell. In this technique, the micropipette is extended to the surface of a cell, and a small negative pressure is applied to create a tight seal between the cell and the tip

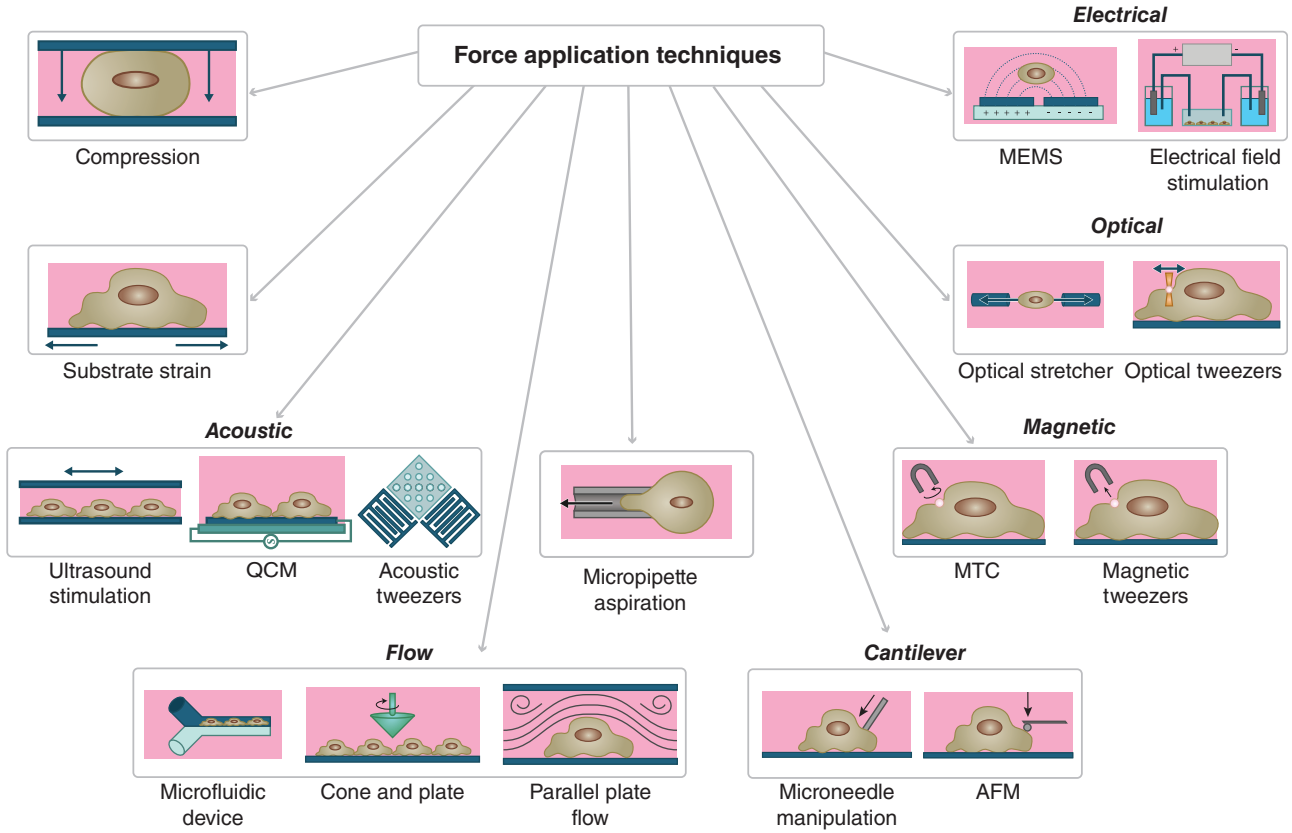

FIG. 2

Force-application techniques for single cells. *QCM*, Quartz Crystal Microbalance; *AFM*, Atomic Force Microscopy; *MTC*, Magnetic Twisting Cytometry; *MEMS*, Microelectromechanical Systems.

of the micropipette. Once this seal is formed, a known negative pressure is applied inducing cell deformation or "aspiration." Micropipette aspiration is used to study whole-cell mechanics by investigating how much cellular material is pulled into a glass pipette in response to the known negative pressure applied. Video microscopy is used to monitor the volume of cell material outside the pipette by tracking the change in radius of material and the height of cellular material inside the micropipette [25,26]. The Young's modulus of the cell can be calculated from the applied vacuum pressure, the length of the cell inside the pipette, and the inner radius of the pipette, if the cell is assumed to be a solid homogenous material [27]. If the cell is assumed to behave as a viscous solid, the cell viscosity can be calculated from these aforementioned values, the radius of the spherical portion of the cell outside the pipette, and the lengthening rate of the cellular material within the pipette [26,27]. The device can measure piconewton-level forces [27]. This technique has been used to determine the elastic modulus and viscoelastic properties of various cell types throughout the years [26,36,37]. It has been extensively used to measure cells in suspension [38–43] but more recently has been used to measure cells adhered to a substrate [44,45]. This technique has also been used to investigate the stiffness of nuclear mechanics by gently isolating the nucleus from the cell cytoplasm [41,46].

2.2 CELLULAR INTERACTIONS WITH THEIR LOCAL ENVIRONMENT

In addition to the investigation of cells themselves, forces generated by the cell in their local environment are key in the study of mechanobiology and tissue engineering. Forces are produced by cells during development, contraction, migration, and other common cell processes [26]. Contractile cellular forces (cellular tractions) are transmitted to other cells via cell-cell interactions and to the local extracellular matrix (ECM) through cell-matrix interactions. These forces generated by cells drive the bending, stretching, alignment, and repositioning required for tissue development and homeostasis, and they also regulate cell functions ranging from receptor signaling and transcription to differentiation and proliferation. Cell tractions are in the range of pico- to nanonewtons and occur across small-length scales (nano- to micrometers), making direct measurement a particularly challenging task. Exciting research in the nascent fields of microfluidics and organ-on-a-chip technologies provide the promise of studying cell mechanobiology in a tailored 3D microenvironment, more closely replicating the physiological and mechanical environment in vivo. These interesting new techniques combine much of the methods described in this section, and detailed reviews can be found elsewhere [46a,46b,46c,46d]. Methods for measuring cellular forces include collagen contraction, tissue pillars, two-dimensional (2D) and three-dimensional (3D) traction force microscopy (TFM), and micropillar arrays. For a review of these methods, refer to Polacheck and Chen [47]; TFM and micropillar arrays are discussed briefly below.

2.2.1 Techniques to analyze cellular tractions

2.2.1.1 Traction force microscopy

Cellular TFM developed by Dembo and Wang [48] remains the most widely used method to measure cell forces. Traction forces generated by cells can be decomposed into a component acting parallel to the substrate surface and a normal component, which acts perpendicular to the substrate surface. The forces that act parallel to the substrate surface generate deformations in the optical viewing plane and can be visualized using wide-field microscopy. TFM involves tracking synthetic elastic polymer substrates as they move in response to cellular forces [47]. Briefly, standard 2D TFM involves mixing small fluorescent beads ($<1\,\mu m$) into a substrate and seeding cells on/in the substrate. The substrate used for this application must be a flat, deformable material that has well characterized mechanical properties. The material must behave as an isotropic linear elastic material under deformations that are likely to occur. In addition to this, the substrate must be resistant to degradation in order to decouple force measurements from changes in mechanical properties of the substrate. The fluorescent beads are optically imaged in a stressed state, and then, the cell traction forces are released by cell lysis, detachment, or myosin inhibition, and the beads are tracked in space and time to determine their position in an unstressed state. Computational algorithms are then used to determine the displacement of the beads from the images and the force required to cause such displacements. This technique allows cellular forces to be mapped at a subcellular resolution as the size of the beads is much smaller than the size of the cells. However, complicated computation calculations are required to determine bead displacements and forces [47]. Various computational techniques are discussed in detail in the following publications [49–51].

Tracking substrate deformation in a 2D plane (as described above) is not representative of a 3D environment as contractile forces generated by cells are distributed throughout the 3D space. For this reason, TFM techniques have been modified to track bead displacement in 3D with confocal microscopy. However, computing traction forces in 3D requires considerable computational resources. Measuring tractions of cells in 3D is difficult for two main reasons: (a) the experimental/computational complexities and (b) the mechanical properties of biologically relevant 3D culture substrates are much more complicated than those of well-characterized nondegradable synthetic materials used for 2D TFM [47].

TFM and related techniques have enabled characterization of the force dynamics involved in a variety of cell biological processes such as adhesion maturation [52,53], migration [48,54–56], differentiation [57], and malignant transformation [58]. Although great progress has been made in this field over the past number of years, it still remains unclear how forces measured in vitro on mechanically simplified materials relate to forces in living tissues. Current methods measure the forces between a cell and a single material, but in vivo, cells are connected to a host of materials and other cells, all of which contribute to the generation and propagation of cellular forces [47]. However, the ever-growing community of engineers, mathematicians, and scientists are working on the continual development of solutions to overcome the shortcomings of current methods.

2.2.1.2 Micropillar arrays

Micropillar arrays are another method to measure cellular traction forces. In this technique, single cells are seeded onto an array of micron-sized evenly distributed pillars/cantilevers. The tops of the cantilevers serve as the cell substrate, which results in a high density of force sensors beneath a single cell. Cellular- or subcellular-scale pillars are typically 0.5–10 μm. The displacements of each cantilever in an array can be tracked, and the observed displacements can be used to calculate the tissue traction forces using beam theory [25,47]. Furthermore, these posts can be fabricated in a cost-effective manner, as described by Rodriguez et al. [26]. Micropillars are also known as micropost arrays or microfabricated postarray detectors (mPADs) [26,47]. Micropillar arrays have been used to investigate cell spreading [59,60], migration [61–63], contractility [60,64,65], focal adhesion strength [66], and cadherin junction tractions [67,68].

2.3 BIOREACTORS TO MIMIC THE IN VIVO ENVIRONMENT

In the body, the forces experienced by tissues and cells vary in both type and magnitude depending on the physiological location. As a result, each type of tissue construct (skin, bone, cartilage, tendon, blood vessel, etc.) has different requirements, making bioreactor design a complex task. For this reason, tissue-specific bioreactors have been developed based on a thorough understanding of biological and engineering aspects, to generate loading conditions in vitro similar to those experienced by cells in their native niche [69]. A tissue-engineering bioreactor can be defined as a device that uses mechanical means to influence biological processes [70]. Bioreactors are generally designed to perform at least one of the following functions: (a) provide a spatially uniform cell distribution, (b) maintain the desired concentration of gases and nutrients in culture medium, (c) facilitate mass transport to the tissue, (d) expose the construct to physical stimuli, and/or (e) provide information about the formation of 3D tissue [71–73]. Numerous studies have demonstrated that the application of mechanical cues assists in the differentiation and growth of stem cells and the production of functional ECM, such as aligned tendon [74–77], cartilage [78–81], and mineralized bone [52,82–84]. Bioreactor studies are often combined with computational/mathematical modeling to advance the understanding of the dynamic environment.

2.3.1 Types of bioreactors

Bioreactors range from advanced commercial systems to custom-built systems developed and built by researchers. Bioreactors have been specifically developed to apply mechanical stimulation via compressive loading, tensile strain, hydrostatic pressure, shearing fluid flow, or indeed a combination of these elements. These types of bioreactors are shown in Fig. 3. For a more thorough review, refer to Pörtner et al. [69].

Flow perfusion bioreactors are most commonly used as they replicate a dynamic environment by allowing 3D structures to obtain nutrients and eliminate waste. Flow

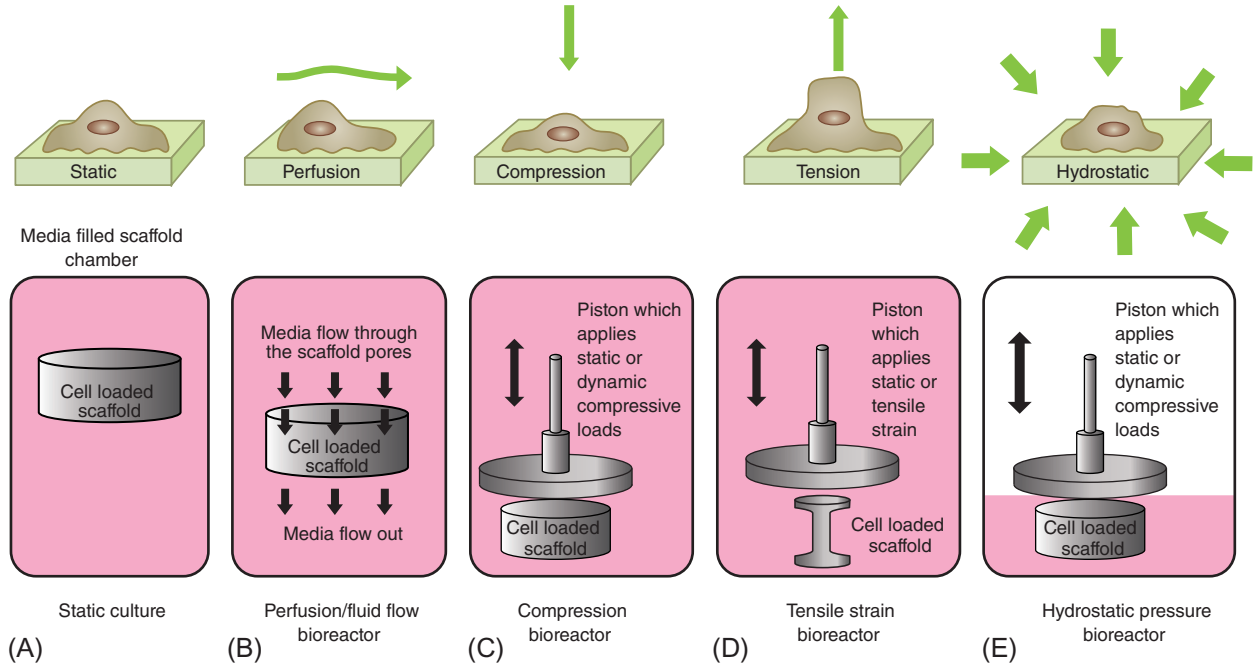

FIG. 3

Static culture (A) and perfusion (B), compression (C), tensile (D), and hydrostatic (E) forces applied to cell loaded scaffolds using bioreactors.

perfusion bioreactors generally consist of a pump that forces the media through a scaffold (located in a scaffold chamber) at a quantifiable flow rate. Media can be easily changed in this experimental setup; however, results may largely depend on the flow rate. Microfluidics systems typically consist of cells grown on a porous scaffold or flat surface, and fluid is pumped across the cell layer, whereas in microcarrier systems, cells are seeded on a scaffold that is placed in an agitated solution [69,71].

Compressive forces in vivo generate shear stress and strain as fluid is forced from the compressed area to the interstitial spaces. Both static and dynamic forces occur in vivo. Compression bioreactors are particularly important in the musculoskeletal system; specifically, osteocytes and chondrocytes are particularly sensitive to compressive forces. Generally, compression bioreactors consist of a motor that provides a linear motion and a controlling mechanism providing displacement regimes. The compressive force is transferred to the construct by flat platens that distribute the load evenly. Mass transfer is usually improved in dynamic compression bioreactors as compression causes fluid flow through the scaffold [71,85].

Tensile forces are commonly experienced in tendons, ligaments, and muscles. In order to grow these tissues in vitro it is necessary to align the cell growth along the appropriate axis. Once the cells are aligned, the intracellular cytoskeleton and ECM deposition will also be aligned parallel to the strain axis. Many tensile strain bioreactors have very similar design to compression bioreactors, differing only in the direction in which the load is applied. In this case, the scaffold is clamped in position using nonslip grips, and tensile strain is applied [69,71].

Hydrostatic pressure bioreactors can be used to apply mechanical stimulus to cell-loaded constructs and are commonly used in cartilage tissue engineering. Hydrostatic pressure bioreactors generally consist of a scaffold chamber that can withstand the pressure applied and a means to apply the pressure, such as an actuator-controlled piston. In this case, the piston must apply the pressure via an impermeable membrane so as not to sacrifice sterility of the experimental setup [71].

The four basic steps of bioreactor design are (a) identifying the needs and technical requirements, (b) defining and evaluating the related concepts, (c) designing and drawing the device, and (d) building and validating the device. Furthermore, the design has to be adapted to the specific purpose of the research and how the tissues will be used [86]. A description of bioreactor design requirements is provided by Partap et al. [71].

2.3.2 Future of bioreactors

Static culture conditions do not accurately represent the dynamic in vivo environment and are being gradually replaced by bioreactor culture systems. A better understanding of the mechanobiological environment of cells in 3D is required for the successful fabrication of functional engineered tissue. Bioreactors are a vital cog in the transition to the next generation of cell research, whereby readily available, easy-to-use systems will allow researchers to apply appropriate mechanical loading to their experiments and hence mimic the native cell environment [87]. However, currently, most bioreactors are specialized devices with a low-volume output. Many

exhibit operator-dependent variability, and their assembly is time-consuming and labor-intensive [71]. First, bioreactors are required to enable us to study this complex 3D environment, and following on from this, scaled-up automated bioreactors are required to produce this engineered tissue.

2.4 ANIMAL LOADING MODELS

Animal loading models are often required to elucidate the mechanobiology of a living tissue under normal and altered mechanical conditions. These models are commonly used to study bone mechanobiology, as loading is particularly important for bone development, remodeling, and regeneration. The bone is constantly remodeled by the coordinated action of bone-resorbing osteoclasts and bone-forming osteoblasts. During physical activity, mechanical forces are exerted on bones through ground reaction forces and by the contractile activity of muscles [88,89]. These physical forces result in a maintenance or gain of bone mass and adaptive bone remodeling. The lack of physical activity/mechanical loading results in resorption of the bone [90]. Numerous animal loading models have been developed throughout the years to test specific hypothesis about bone modeling and remodeling. Animal loading models are used to apply forces at the organ scale in order to generate responses at the cellular level in an effort to determine what mechanical signals elicit specific cellular responses.

In a controlled experimental environment, the force required to generate these mechanical signals can come from intrinsic sources, such as voluntary muscle contraction during a vigorous exercise session (noninvasive), or from normal activity following the surgical removal of a nearby bone that formerly shared the load (invasive). Alternatively, the load can originate from extrinsic sources, such as pressure applied to the skin adjacent to the bone (noninvasive) or loads applied to surgically implanted pins (invasive) [91]. For a review of some of the most widely used animal loading models for bone, refer to Robling et al. [91]. While we focus here on skeletal tissues, animal models have been applied in mechanobiological studies of a number of other organs, for example the tendons in mouse treadmill running (described in Chapter 5), the vasculature of hypertensive mice (described in Chapter 7) and scar mechanotransduction in pig skin tissue (described in Chapter 14).

2.4.1 Noninvasive extrinsic skeletal loading models

Early models enabling extrinsic control of load levels provided a significant insight into bone remodeling; however, they typically employed invasive surgical procedures, which can present complications (e.g., infection and inflammation) in experiments and interpretation of results. This led to the development of noninvasive animal loading models that are capable of applying a well-defined mechanical signal to the bone without the potential complications of surgery. Noninvasive models are technically simpler, less expensive and do not rely on healing processes, as compared with the surgical models [91]. The two most commonly used noninvasive animal

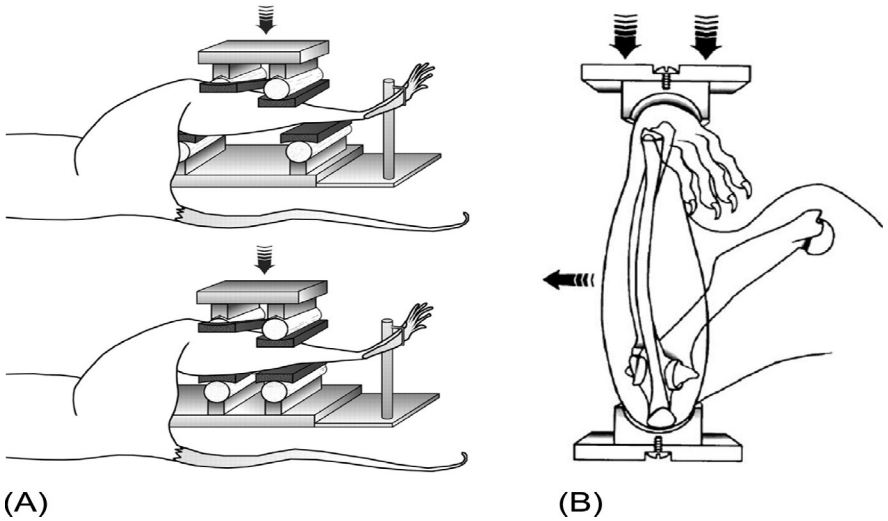

FIG. 4

Skeletal animal loading models. (A) Tibial four-point bend model [94]; (B) ulnar compression model [15].

loading models are the tibial four-point bending approach developed by Turner and coworkers [92] and the ulnar compression model of Lanyon and coworkers [93].

2.4.1.1 Tibial four-point bend model

The tibial four-point bend model was first described by Turner [92], whereby the rat tibia is subjected to four-point bending in the mediolateral direction. The right hind limb of an anesthetized animal is placed between pairs of upper and lower padded load points. A downward force is applied to the upper points, and the load is transmitted to the tibia through the skin, fascia, muscle, and periosteum, resulting in the production of a bending moment in the region between the two upper points. The bending moment imposes a compressive strain on the lateral tibial surface and tensile strain on the medial surface, as shown in Fig. 4A (top). On the contralateral leg of the animal, a sham configuration is implemented, whereby the upper and lower points directly oppose each other, as shown in Fig. 4A (bottom). In this configuration, the sham leg is squeezed, but the bone does not deform [95]. This model has since been scaled down for a mouse model [96].

2.4.1.2 Ulnar compression model

In the ulnar compression model [93], the forearm of an anesthetized animal is secured between two small metal cups that are mounted on the platens of a materials testing machine or other actuator. The elbow is secured with one cup, and the dorsal surface of the volar-flexed wrist is secured in the second cup. Compressive forces applied to the platens are transmitted to the ulnar diaphysis through the skin, fascia, articular cartilage (at the distal end), and ulnar metaphyseal bone, as shown in Fig. 4B.

The natural curvature of the ulnar diaphysis translates ~90% of the axial compression into a mediolateral bending moment [91]. The ulnar loading model was also initially developed for the rat and has been modified for the mouse [97] and rabbit [98].

In both the tibial four-point bend model and the ulnar compression model dynamic loads are applied, and the load magnitude, rate, number of cycles, and duration are well controlled. These noninvasive models, combined with increased computing power, higher resolution imaging, and new molecular techniques, will enable systematic evaluation of loading parameters to understand the nature of the osteogenic stimuli and pathways [99]. Additionally, the explosive growth of transgenic animal technology will undoubtedly lead to a more comprehensive understanding of the process of mechanically induced bone formation.

2.4.2 Embryonic animal models with an altered mechanical environment

Evidence from animal models has been key to help our understanding of the importance of movement as a regulatory tool in sculpting skeletal development. In animal models, the mechanical environment can be altered in a number of ways including the in vivo immobilization of the musculature (in ovo immobilization) or the use of mutant mouse embryos in which the skeletal rudiments develop with reduced, absent, or noncontractile muscle (reviewed in Ref. [100]). Both the chick and mouse are valuable vertebrate models used to investigate the effect of mechanical stimulation on embryonic skeletal development, due to their similarities with human musculoskeletal development.

2.4.2.1 In ovo immobilization

An advantage of the chick embryonic model is that it can be physically manipulated in ways that are impossible in the mammalian embryo. The chick shares many features of embryonic development with mammals and has a huge advantage of development external to the mother, in ovo (in the egg), which allows procedures and alterations to the embryos and resulting effects to be examined (reviewed in Ref. [101]). During chick development, innervations of chick myotomes occur at approximately embryonic day 3 (E3) [102], and it has been reported that spontaneous limb movements occur from E3.5 to hatching [103]. Immobilization can be achieved in the developing chick embryo either surgically, by extirpation of the spinal nerves, or by application of pharmaceutical agents that block neuromuscular signals (e.g., Refs. [104–106]). Immobilization studies on the chick have shown that biophysical stimuli are required for correct initiation of ossification [104], several aspects of joint morphogenesis [105,107–110], and correct spine development [106].

2.4.2.2 Mammalian models

Essential information about regulatory genes and the role of environmental stimuli for skeletal development has emerged using the developing chick model; however, for appropriate comparison with human development, the mammalian murine model has been utilized. Another benefit of the murine model is the substantial knowledge of the genome and the similarity in gene regulation mechanisms with the human. Muscle contractions begin relatively early in development, at approximately the

same time as the cartilage template is taking shape, after approximately E12.5 in the mouse [111]. Genetic manipulation has produced mouse models that can be used to study the effect of mechanical stimulation from movement on skeletal development; they include mice with reduced (*Myf5*$^{nlacZ/+}$:*MyoD*$^{-/-}$ [112]), immobile (Mdg$^{-/-}$ [113]), or absent (*Splotch* [114,115], *Splotch delayed* [116,117], *Myf5*$^{nlacZ/nlacZ}$:*MyoD*$^{-/-}$ [118,119], *Six1*$^{-/-}$:*Six4*$^{-/-}$ [120]) skeletal muscle. These mouse models that lack normal muscle contraction show similar skeletal phenotypes to those observed in the chick immobilization studies including joint fusions and alterations in the ossification pattern [121].

2.4.2.3 Zebrafish models

The recent emergence of the zebra fish as a model for mechanoregulation of the skeletal system builds on the work of the previously described chick and mouse. The zebra fish is a system, however, in which many transgenic lines are available, specifically those that mark the various cell types of the musculoskeletal system [122]. This system has aided the understanding of cellular behavior following the manipulation of the mechanical environment [123]. Paralysis of the zebra fish exhibits a reduction in the size of all pharyngeal cartilage, establishing muscle loading in this model as a regulator of chondrocyte intercalation [124]. Similarly, zebra-fish mutants that lack neuromuscular nicotinic receptors (*nic* b107) and are therefore immobile display jaw morphology abnormalities, such as smaller and wider elements [124]. Both flaccid and rigid paralysis of the zebra fish have been shown to show similar changes to the morphology and function of the jaw joint [125]. It has recently been demonstrated using live zebra-fish joint imaging that cell behavior such as proliferation, migration, intercalation, and cell morphology changes required to shape the jaw joint are altered under reduced biomechanical conditions [126]. The malleable nature of this model could potentially hold promise for joint malformation recovery studies following periods of immobilization, as may occur in utero.

2.5 FLUORESCENT PROTEINS (FPs) AND IMAGING TECHNIQUES

The discovery of green fluorescent protein (GFP) in 1962 [127] has led to the development of a number of FPs with various hues. FPs are members of structurally similar class of proteins that share the unique property of emitting fluorescence at a specific wavelength when excited by a specific wavelength. FPs can be fused to virtually any protein of interest and genetically encoded into cells to analyze protein geography, movement, and chemistry in living cells [128]. FPs have been widely used for live-cell imaging over the past 20 years and have advanced our understanding of many important molecular and cellular functions in live cells. For a thorough review on the various FPs, refer to Wang et al. [129]. As a result of the innovation in FPs, new imaging technologies that utilize FPs have also been developed. Techniques utilizing novel FPs and imaging technology have been making a substantial impact on mechanobiology research over the past number of years.

2.5.1 FPs as markers in mechanobiology

Mechanical forces can activate a number of signaling molecules located in the cell membrane and other subcellular compartments. As FPs are genetically encoded, they are well suited for the imaging of the spatiotemporal localization and activation of signaling molecules and structures in live cells in response to mechanical stimuli. A large number of signaling molecules have been labeled with FPs, and as such, the position and movement of these molecules can be visualized with high spatiotemporal resolution techniques [129,130]. FPs and live-cell imaging can be used to visualize organelles, cytoskeleton, signaling molecules, and gene expression in mechanobiology, as discussed in detail by Wang et al. [129].

Briefly, at the organelle level, FPs can be fused to signaling molecules that localize to subcellular organelles to monitor where the organelle resides. FPs can highlight organelles to serve as reference points for the determination of the global mechanical properties [131–133]. FPs can also be fused to cytoskeleton molecules such as actin, microtubules, and intermediate filaments making the cytoskeleton fluorescent whereby morphology and deformations of the cytoskeleton can be monitored in a dynamic fashion [134,135]. Labeling and monitoring the dynamics and intercompartmental traffic of signaling molecules have been the most successful use of FPs in mechanobiology to date. FPs have been used to observe the molecular dynamics in terms of intracellular mechanical tension/stress [136–138], extracellular mechanical environment [139,140], external mechanical loading [141–144], and the mechanical impact the cells exert on the extracellular environment [52,53]. FPs have also been used to investigate the translocation of specific target molecules among different subcellular organelles [145–148]. In gene expression, FPs are fused to the promotor region of the gene of interest; when cells are exposed to various types of mechanical stimulation, the up-/downregulation of the gene can be monitored by the levels of expressed FPs [129].

2.5.2 Imaging technologies using FPs

2.5.2.1 Live cell imaging

Time-lapse imaging is used to observe and capture cellular dynamics by imaging live cells at regular time intervals using fluorescent or indeed light microscopy. In this technique, a camera captures sequences of images that are later viewed at faster speed to track cellular responses over time. The two main experimental challenges in collecting robust live-cell imaging data are to minimize photodamage while retaining a useful signal-to-noise ratio (specifically for fluorescent imaging techniques) and to provide a suitable environment for cells or tissues to replicate physiological cell dynamics. Living cells will only behave normally in a physiological environment, and control of factors (temperature and cell culture medium) using an environmental chamber is therefore critically important. The single most important factor to successful live-cell imaging and meaningful data is to limit excitation light as photobleaching is inevitable with this technique, as discussed by Ettinger et al. [149].

2.5.2.2 Fluorescent resonance energy transfer (FRET)

Fluorescent resonance energy transfer (FRET) is a phenomenon of quantum mechanics that involves the nonradiative transfer of energy from a donor to an acceptor fluorophore (molecule that fluoresces) [129]. A fluorophore can serve as a FRET donor if its emission spectrum overlaps the excitation spectrum of another fluorophore, the acceptor fluorophore. When the donor and the acceptor are in close proximity to one another (<10 nm) at the correct orientation, the excitation of the donor can elicit an energy transfer, inducing emission of the acceptor. FRET efficiency is defined as the proportion of the donor molecules that have transferred excitation state energy to the acceptor molecules and is dependent on the distance and orientations between the fluorophores. FRET is a reversible reaction and occurs instantaneously [129]. Genetically encoded FRET biosensors can be easily introduced into cells making this technique well suited to molecular live-cell imaging to monitor mechanotransduction with high spatiotemporal resolutions. FRET-based techniques have been employed to visualize signal transduction in response to mechanical stimulation, as discussed by Wang et al. [129]. Briefly, Chachisvilis et al. [150] fused ECFP and EYFP (fluorescent proteins) to human B_2 bradykinin receptor, a G-protein-coupled receptor (GPCR), to detect the activation of GPCR. Using FRET, they showed that shear stress activated B_2 bradykinin in bovine aorta endothelial cells, and this effect can be inhibited by B_2-selective antagonist. These results suggest that the membrane B_2 bradykinin GPCRs are involved in mediating primary mechanochemical signal transduction in endothelial cells [150]. More recently, FRET has been reported in 3D where Zhao et al. demonstrate that Ca^{2+} and cAMP levels of live embryos expressing dual FRET sensors can be monitored simultaneously at microscopic resolution [151].

2.5.2.3 Fluorescent recovery after photobleaching (FRAP)

Fluorescent recovery after photobleaching (FRAP) is a technique where fluorescent signals are selectively photobleached within a subcellular region, and the recovery of the fluorescence is monitored in that region over time. The fluorescent intensity of the bleached area will recover at different rates, depending on the levels of diffusion and active transportation of fluorescent molecules [129]. FRAP has been widely used to investigate molecular dynamics in mechanobiology. Using FRAP, Vereecke et al. [152,153] assessed the speed of intracellular Ca^{2+} wave propagation during mechanical stimulation in rat retinal pigment epithelial cells. FRAP has also been used to show that mechanical stress controls the focal adhesion assembly by modulating the kinetics of zyxin in bovine adrenal capillary endothelial cells [136].

2.5.2.4 Confocal and two-photon microscopy

Cells in their native 3D environment behave very differently to in vitro 2D cultures [154–156]. Investigation into cellular responses requires 3D images at the cellular, subcellular, and ultrastructural levels. Imaging structures in 3D is an inherently difficult task as the contribution of a signal from above and below the focal plane produces background fluorescence, affecting the quality of the image. Depths and

scattering effects [156] require new imaging techniques to achieve high-resolution images of cells and indeed FPs in 3D environments.

In confocal laser scanning microscopy, a point-source laser light excites a fluorophore in the sample that either is autofluorescent or has been stained with specific fluorescent dyes. The sample is imaged at sequential focal planes, and a pinhole detector excludes out-of-focus background fluorescence from detection. A stack of 2D optical sections is acquired, which enables production of 3D representations of internal structures [157]. However, in this technique, as the excitation light generates fluorescence, it also produces photobleaching and phototoxicity throughout the specimen (even though the signal is only collected from the plane of focus). The penetration depth is also limited by absorption of excitation energy throughout the beam path and by specimen scattering of the photons [157–159].

Two-photon excitation microscopy has been developed as an alternative to conventional single-photon confocal microscopy. In two-photon excitation microscopy, a fluorophore is excited by the simultaneous absorption of two long wavelength (low energy) photons. In this case, their combined energy induces excitation of a fluorophore, which normally requires the absorption of a high energy to become excited. This can only occur at a very focused area with limited volume (femtoliter scale) [129], and as such, noise originating from the areas outside the focal region is eliminated. As a result of the enhanced signal-to-noise ratio, the penetration depth of imaging is improved (several hundred micrometers) without significant photobleaching [129,160,161]. As this technique enables increased depth penetration and can be less phototoxic to live specimens, it has been widely used at the molecular, cellular, tissue, and animal levels [162–165,165a,165b].

3 MOLECULAR AND GENETIC TECHNIQUES TO STUDY MECHANOBIOLOGY

3.1 ANALYSIS OF mRNA EXPRESSION

To understand how a biological system works, researchers seek to comprehend the functioning of the systems' component parts. As all cells in a given organism possess an identical genetic makeup, it is the unique phenotypes or observable characteristics directed by differential gene expression that guide the system's complexity. The first step to understanding this complexity in assorted cell types is to discover which genes are expressed by the cells of interest, thus guiding cellular differentiation into specific tissue types and then into functioning systems. Great progress has been made over the recent years toward understanding the role that mechanical stimulation has on the development and maintenance of tissues and the impact it has in guiding cell differentiation [100,166,167]. Much of this understanding of the integration of mechanical forces and cellular responses has been possible through the analysis of messenger RNA (mRNA) profiles and changes in gene expression following alterations in the mechanical environment. The central dogma of molecular genetics is

that DNA codes for protein not directly but indirectly through processes called transcription and translation. This indirect route of information transfer involves an intermediate ribonucleic acid (RNA) molecule that relays the message. This so-called mRNA carries the genetic information transcribed from DNA and is used to translate a template for protein synthesis. Through the analysis of mRNA by different means, as discussed below, it is possible to understand the types of proteins that are being guided to be produced by this molecular information transfer.

The objective of this section is to provide researchers from traditional engineering backgrounds with the theoretical principles and practical techniques of experimental molecular biology, to utilize in the field of mechanobiology.

The first step in selecting a method of mRNA expression analysis is to assess whether a hypothesis can be tested using known specific genes that may be responsive to experimental mechanical manipulation. In these cases, methods of detection of specific individual/single genes would be appropriate. Techniques for individual-/single-gene expression include in situ hybridization (spatial expression) and quantitative real-time polymerase chain reaction (qRT-PCR). In cases when specific gene changes would be unknown, a more high-throughput screening approach using techniques such as microarray or RNA sequencing that focus on genome-wide patterns of gene expression would be more appropriate. Utilizing high-throughput methods of mRNA detection offers the benefit of simultaneously capturing changes in interacting groups of genes, with the potential of illustrating novel mechanisms of mechanotransduction. This section will present the basic principles underlying the molecular and genetic techniques of high-throughput and individual-level detection of mRNA expression that have been utilized for mechanobiology studies.

3.1.1 Microarray analysis

DNA microarray or chip-based detection was the first of its type to take a large-scale screening approach to collect large data sets to allow data mining and reveal intricate functions. The methodological approach was originally used for sequence analysis but then became widely adopted to quantitatively measure changes in gene expression (reviewed in Ref. [168]). Microarray technology works on the principle of nucleic acid site-specific sequence binding or hybridization onto synthetic sequences present on a chip. A microarray (or chip) is a flat surface in which 10,000–100,000 distinct oligonucleotide (short number of nucleotides) probes are present. These probes represent unique sequences for individual genes that will allow for complementary binding of mRNA from cell/tissue samples. For both in vitro and in vivo experiments involving alterations of the mechanical environment, separate control and experimental groups are formed. The method includes total RNA extraction, reverse transcription of the RNA using oligo-dT primers, and inclusion of a promoter sequence. In vitro transcription is then performed to form complementary DNA (cDNA) incorporating a fluorescent label. The fluorescently labeled cDNA is hybridized with the microarray (chip), to allow the complementary sequence-specific binding of the sample cDNA with the oligonucleotide probe sets on the chip. Following rinsing and digital scanning of the chip, the abundance of RNA (bound labeled

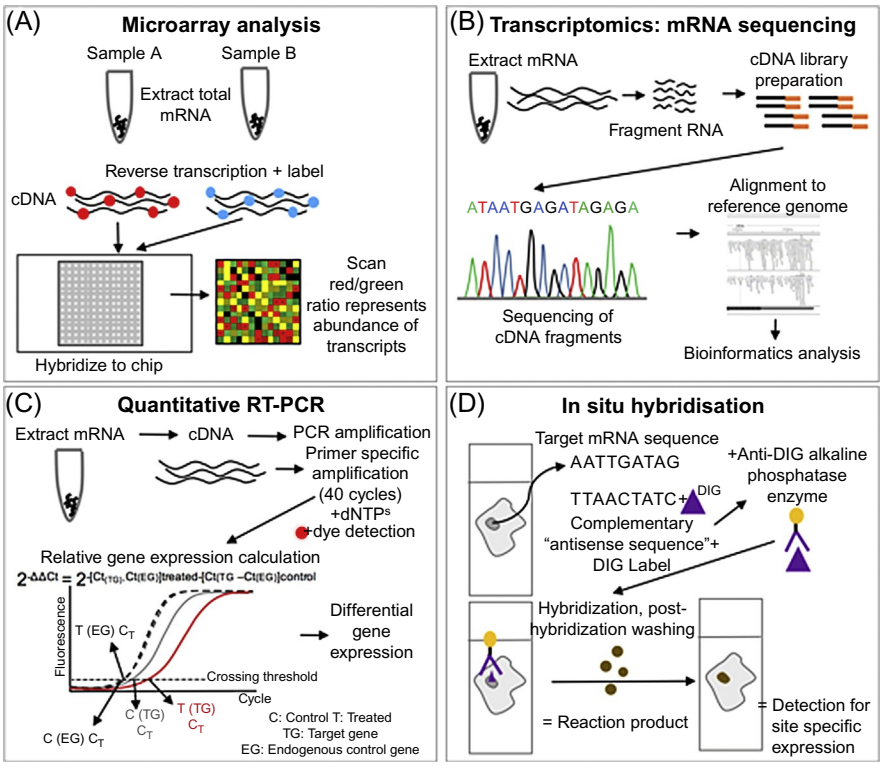

FIG. 5

Molecular techniques using mRNA expression to analyze mechanobiology. Basic flow through of each technique as described in the text for both high-throughput identification of changes in gene expression using microarray analysis (A) and transcriptomic mRNA sequencing (B) and more individual- or single-based gene expression changes using quantitative RT-PCR (C) and in situ hybridization (D).

cDNA) is determined by measuring fluorescent density (Fig. 5A). Data are then normalized among replicates for control and experimental groups and the statistical analysis performed. Differential gene expression is generally indicated with a fold change of $\geq$2.0 or $\leq$2.0.

The molecular response following alterations in the mechanical environment has been reported in various in vitro and in vivo studies in an attempt to understand in more detail the means by which mechanical stimuli modulate the cellular response during cellular differentiation. Profiling of genome-wide changes under altered mechanical environments has been carried out using in vitro culture systems in conjunction with microarray technology, including osteoblast cell lines subjected to weightlessness or microgravity conditions [169] and chondrocytes subjected to anabolic loading [170], dynamic compression [171], or hydrostatic pressure [172].

Analysis of genetic responses to altered mechanical environment during in vivo conditions has also been performed, including expression changes to an absence of movement during embryonic limb development [173].

A limiting factor of the hybridization methodology is its high background, because it is unable to distinguish RNA molecules sharing high sequence similarity. Microarrays also rely on hybridization with a labeled probe in which sequence is known, while RNA-sequencing technology doesn't depend on the genomic sequences being known that allows the potential to identify novel gene sequences.

3.1.2 Transcriptomics: Total RNA and mRNA sequencing

A transcriptome is the whole set of RNAs transcribed by the genome from a specific tissue or cell type at a particular developmental stage and/or under a certain physiological condition. Following the sequencing of the genome, transcriptome analysis allowed researchers to understand further information on gene structure and regulation of gene expression. This technique has been utilized in multiple aspects of biology to reveal the regulation network of biological processes and guidance on aspects of diseases and drug discovery [174–176]. Transcriptome sequencing is a major advance in the study of gene expression because it allows a snapshot of the whole transcriptome rather than a predetermined subset of genes. Direct comparisons between RNA-sequencing-based approaches and microarray technologies to reveal alterations in gene expression between tissues report that RNA-seq identifies a great number of differentially expressed genes [173,177–179] and is more sensitive in reproducibly detecting alterations in gene expression at lower quantitative levels [173].

The steps for RNA sequencing begin in the same way as for a microarray, and total RNA is extracted. This RNA is then converted into a library of cDNA fragments. Sequence adaptors are added to each cDNA fragment, and a short sequence is obtained from each fragment from one end (single-end sequencing) or both ends (paired) using high-throughput sequencing technology (reviewed in Ref. [180]). The resulting sequence reads are aligned with the reference genome or transcriptome, or in the case where there is a limited reference genome, they can be assembled to produce a genome-scale transcription map that consisted of level of expression for particular genes (Fig. 5B).

This technique has advanced greatly over the last 10 years and is overcoming challenges with respect to cDNA library construction, bioinformatics, and sequence coverage versus cost (reviewed in Ref. [180]). A factor to consider when utilizing this technique for expression analysis is the quantity of high-quality RNA available for analysis. Recent work has optimized a protocol to extract high-quality RNA from human articular cartilage and performed RNA-seq; this advancement could be valuable to understand more about expression changes in osteoarthritic patients [181]. More recent advancements in the next-generation sequencing field have seen the emergence of single-cell RNA-sequencing technology (scRNA-seq) that is designed to overcome population-averaged RNA-seq that may mask rare subpopulations of cells (such as stem cells). Single-cell RNA-seq attempts to investigate expression

profiles at the cell level, and comparisons between tube- and microfluidic-based extraction methods are being explored [182,183]. The advancement of single-cell genomics had the advantage of exploring cellular process with a more accurate resolution and thus may be of benefit to understanding mechanotransduction events in multiple contexts.

3.1.3 Quantitative real time PCR

qRT-PCR is a technique that is comprehensively used to analyze the expression levels of individual gene transcripts in a particular tissue or cell population following environmental manipulation. PCR was first devised in 1985, and it has had a major impact on biological research and genetic engineering. Through which, it is now possible to analyze 40,000-year-old DNA, DNA from fingerprints, blood, and tissue found at crime scenes, and analyze single embryonic cells for prenatal diagnosis of genetic disorders and virally infected cells. It is no doubt that this technique has been invaluable to our understanding of mechanobiology and the analysis of cellular changes following a change in the mechanical environment. qRT-PCR begins by converting sample mRNA into cDNA with corresponding sequences (using reverse transcriptase and DNA polymerase). PCR amplification is then performed encompassing a denaturation step (to separate DNA strands), an annealing step (to allow known sequence-specific primers for a particular gene to bind to the ends of the target sequence), and an extension phase (when DNA polymerase adds free nucleotides to the end of each primer). These steps are then repeated up to 40 cycles, which results in an exponential growing population of identical DNA molecules. Inclusion of a fluorescently bound dye during the annealing phase that fluoresces only when bound to a double-stranded PCR product is read computationally, and the levels of expression or C_t (cycle threshold) value for a particular gene can be quantified. The cycle threshold method [184] is an example of the relative quantification approach that compares a gene of interest between experimental and control samples, following normalization to an endogenous control gene (Fig. 5C).

Changes in or identification of mechanosensitive genes following the application or removal of mechanical stimulation commonly utilizes qRT-PCR to confirm high-throughput data output [169,171,173]. The use of qRT-PCR is also valuable in assessing changes in the cellular phenotype following the manipulation of the mechanical environment. Work on mechanisms of chondrocyte differentiation shows that the application of hydrostatic pressure on embryonic cells and adult-derived progenitor cells results in a "stable" cartilage phenotype [185–187]. Work on wound healing identified that mechanical strain results in the upregulation of matrix remodeling genes and the production of more matrix [188]. This technique has also been valuable in revealing changes in gene expression due to changes in the mechanical microenvironment in glaucomatous cells [189] and changes in the thermal environment of bone cells during surgical cutting [190,191]. The value of this approach supports the quantification of the molecular changes in a tissue or cell population; however, it does not show the exact location in which these changes are taking place; this can be addressed with the technique called in situ hybridization.

3.1.4 In situ hybridization

In situ hybridization is a powerful tool for detecting DNA or RNA sequences in intact cells, tissues of whole organisms. Mary Lou Pardue and Joseph Gal pioneered the technique of in situ hybridization by using a radioactive test DNA to label stationary DNA of a cytological preparation [192] (Fig. 5D). This approach allowed for the first time the spatial localization of genetic information. This technique has continued to advance, and the method of complementary binding of a nucleotide probe to a specific target sequence is still applicable, with probes being labeled radioactively, colorimetrically, or fluorescently [193]. In situ hybridization is extensively used in research and clinical applications, especially for diagnostic purposes. Use of this technique has aided interpretation of phenotypic changes following the manipulation of the mechanical environment during skeletal development (Fig. 6A) [104,110,173,194,196] to elucidate the expression profile of genes in mechanosensitive regions [197].

Gene expression profiling at an individual-/single-gene level that has altered the mechanical environment in vivo has investigated candidate genes for altered expression, in order to assess the molecular response to alterations in biophysical stimuli. Both qualitative and quantitative approaches, as described above, to investigate changes in these genes have been performed [104,173,194,196,198,199].

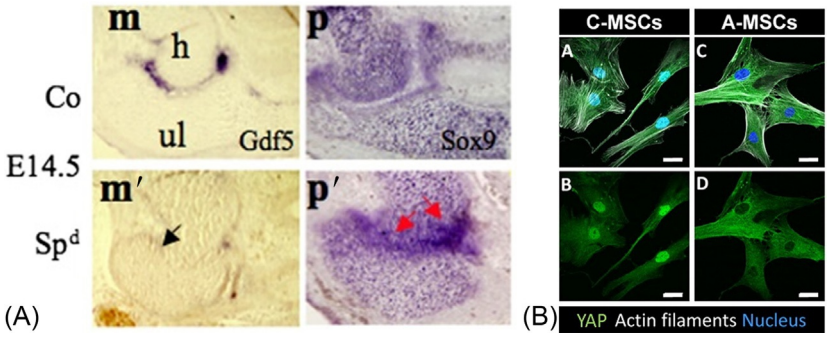

FIG. 6

(A) In situ hybridization shown by Kahn et al. [194] in the developing mouse humeroradial joint at 14.5 days of embryonic development. Sections of control (m, p) and Spd muscleless mutant (m′, p′) show no Gdf5 expression in Spd (*arrow* in (m′)) in contrast to the control joint region (m). *Arrows* indicate joint loss in the mutant as visualized by Sox9 (p′) gene expression (*ul*, ulna; *h*, humerus). (B) Immunofluorescent detection of nuclear or cytoplasmic YAP, shown by [195]. This study investigates the effect of age and substrate stiffness on MSCs on nuclear-to-cytoplasmic location of YAP as a measure of osteogenic mechanotransductive signaling. (A and B) YAP is located in the nucleus of children-derived MSCs (C-MSCs), while (C and D) it is located in the cytoplasm of adult-derived MSCs (A-MSCs) when cultured in control conditions.

Application of various forms of mechanical stimulation during in vitro culture regimes is a major goal of bioengineering techniques in order to create tissue suitable for regeneration applications. Through the methods described, it has been possible to reveal molecular responses to mechanical stimulation and identify tissue compositions due to the known molecular identity profiles.

3.2 ANALYSIS AT THE PROTEIN LEVEL

How cells perceive and relay dynamic mechanical signals to illicit an intracellular response and an alteration at the mRNA transcript level still remains unclear. Other avenues to aid understanding of these changes are at the protein level. It is credible that biomechanics impacts on proteins that guide cell matrix, cell-cell adhesion, and cytoskeletal and ultimately nuclear interactions [200]. This perspective in analyzing mechanobiology has been driven by the recent developments in functional proteomics and the ongoing advances in mass spectrometry quantitation (reviewed in Ref. [200]). More traditional approaches to understanding or observing changes at the protein level include the use of antibodies through spatial localization (immunohisto-/cytochemistry) or enzyme-linked immunosorbent assay (ELISA) or the identification of proteins based on molecular weight (western blotting [201]). The basis of these three techniques relies on a particular antigen-antibody complex binding.

3.2.1 Immunohistochemistry

To identify specific proteins in a tissue or cell type of interest, antibody molecules for specific target molecules are exposed to the sample. The binding of these molecules is detected by incubating the sample with a secondary antibody specific for immunoglobulin molecules and conjugated to a fluorophore (for fluorescent detection). This provides both a visible signal and amplification of the signal that can be visualized using a fluorescent microscope. Immunohistochemistry (IHC) provides information about the spatial localization of protein expression and qualitative evaluation of expression levels. The general steps for the procedure involve fixation, embedding, and sectioning (for tissue samples); detergent permeabilization of cell membranes; antigen retrieval (commonly used for paraffin-embedding sections to increase specificity of binding); and blocking and incubation with appropriate primary and secondary antibodies. Double or triple labeling of antigens can be performed in a single sample, as long as each primary antibody is either a different isotype or raised in a different species so that each can be recognized by distinct secondary antibodies with different labels. Appropriate negative controls are required during the procedure to confirm specificity of staining. A common approach is to use "no primary antibody controls," in which the primary antibody is omitted but the secondary is placed on the sample; this will give insight into nonspecific binding.

The use of IHC in mechanobiology research has facilitated investigation into phenotypic changes in cell populations following the application of mechanical stimulation in vitro [187,202,203]. This technique also provides value for the investigation

of mechanisms of mechanotransduction, for example, through the evaluation of primary cilia following the application of mechanical stimulation [204–206]. The nuclear localization of specific signaling pathway components similarly utilizes this technique, in an attempt to understand how cells sense and adapt to external forces and physical constraints. An example of this is the analysis of the role of the YAP/TAZ (Hippo pathway components) as nuclear relays of mechanical signals exerted by ECM rigidity and cell shape (Fig. 6B) [195,207].

3.2.2 Western blotting

Western blotting (or sodium dodecyl sulfate-polyacrylamide gel electrophoresis (SDS-PAGE)) is a technique that identifies specific proteins based on separation by molecular weight through gel electrophoresis. The theory of the procedure is as follows: sample preparation (most commonly cell lysates), gel electrophoresis (two types of agarose gels: stacking and separating), blotting (electric transfer from gel to a membrane), washing, blocking, and antibody incubation [201]. The signal is then detected from the bound antibody, usually with an enzyme; this then corresponds to the target protein. Normalization among samples and experimental groups is based on the loading of each sample lane with an equal amount of total protein. For further validation, it is common practice to reprobe the membrane for a putatively constitutively expressed protein, such as beta-actin.

3.2.3 ELISA

The most sensitive and quantitative technique for protein analysis, ELISA, allows high specificity, even in complex solutions such as blood. The technique uses a biochemical assay to detect the presence of an antigen in a liquid sample. Since its first description by Engvall et al. in the 1970s [208], ELISA has experienced rapid adoption as a diagnostic tool in medicine, a valuable investigative method in scientific research and a quality control check in various biotech industries. While several different variations of the technique have been developed, the "sandwich" ELISA is the most pertinent and useful for analyzing soluble proteins in scientific research and will therefore be discussed in detail here. A sandwich ELISA operates by using two separate antibodies that recognize different epitopes, which can be either two different monoclonal antibodies or a polyclonal antibody solution. This method allows the measurement of growth factors and/or cytokine levels in cultures or biological liquids, providing convenient assessment of the biological responses to stimuli such as mechanical loading. ELISA kits are commercially available (typically as a 96-well plate), though they can be expensive. It is recommended that for high-throughput experiments for repeated analysis of particular antigens, a custom kit be developed in-house. However, custom sandwich ELISAs used for research purposes should be validated due to the risk of false-positive results [209].

The initial step in a sandwich ELISA involves coating the surface of the wells such that a known quantity of the capture antibody adsorbs onto its surface. Following blocking of any nonspecific binding sites, the wells should be incubated with serially diluted standards of known concentration and experimental samples.

A "blank" group, one without samples or standards, should be included to allow measurement of the background signal in the assay. Next, an enzyme-conjugated detection antibody should be added, followed by a substrate that forms a soluble colorimetric, fluorescent, electrochemical, or chemiluminescent product when cleaved. Between each step, extensive washing should be performed, adding a "stop" buffer at the end of the assay to terminate the enzyme reaction. A plate reader is then employed to collect the raw data, and a standard curve is generated upon removal of the background signal. Given appropriate conditions, ELISA can accurately measure sample concentrations in the low (<10) pictogram/millimeter range, and ELISA data are usually normalized to total protein or DNA (e.g., pictogram antigen/nanogram DNA) in order to account for potential variability in cell number among samples and experimental groups [210]. ELISA kits have been applied to study mechanobiology in varied tissues and organs, for example, exploring the effect of loading on intervertebral disk degeneration [211], examining correlation between pressure and cell stiffness in heart valve cells [212], and incorporating into microfluidic devices to characterize mechanotransduction in vitro [213].

3.3 TECHNIQUES FOR EDITING GENE FUNCTION AND ALTERING THE MECHANICAL ENVIRONMENT

3.3.1 *In vitro mutagenesis—Mice*

A technique called in vitro *mutagenesis* encompasses specific mutations being introduced into a cloned gene, and the mutated gene is returned to a cell in such a way that it disables or "knocks out" the normal cellular copies of the same gene. If the introduced mutations alter or destroy the function of the gene product, the phenotype of the mutant cell may help reveal the function of the missing normal protein. Using molecular and genetic techniques worked out in the 1980s, researchers can generate mice with any given gene disabled in order to study the role of that gene in development and in the adult. Multiple mouse models have been utilized to examine and investigate the role of the mechanical environment on cellular function, some of which are detailed below.

3.3.2 *CRISPR*

The novel molecular technique that has become increasingly popular over the past 5 years based on the identification of the functions of clustered regularly interspaced short palindromic repeats (CRISPR) and CRISPR-associated (Cas) genes and the manipulation of these for genome editing. The functions of CRISPR and Cas genes are essential for adaptive immunity, enabling organisms to eliminate invading genetic material [214,215]. The relative simplicity of the CRISPR nuclease system makes it amenable to adaptations for genome editing, which was realized in 2012 [216]. Manipulation of this system as a tool in molecular biology allows for either gene silencing or activation. To date, this tool has been used in multiple systems, including human, bacteria, zebra fish, and mice (reviewed in Ref. [214]). This tool has recently been utilized to eliminate gene function in a model of tendon biology in

rats, to understand the cellular responses to mechanical stress [217]. CRISPR has the potential to expand our knowledge of the molecular mechanisms that are involved in mechanobiology, and the potential of its use will unquestionably be demonstrated over the next 5–10 years.

3.3.3 In ovo/ex ovo manipulation—Chick

A powerful tool for unraveling the molecular mechanisms involved in developmental processes is to ectopically express a gene or signaling pathway of interest and examine the effect. The avian embryo offers many advantages for developmental studies over mammalian embryos, due to the ease of access for in ovo (in the egg) manipulations. Different types of manipulations can be performed in ovo including surgical and chemically induced immobilization (discussed below). Retroviral transmission has been used very successfully to deliver genes into tissue locations in chick embryos (reviewed in Ref. [218]). Retroviral independent gene transfer can be achieved in chick embryos using in ovo electroporation, a more successful technique for targeting specific embryonic tissues/cells compared with microparticle bombardment and lipofection, offering a positive alternative to broad retroviral infection [219,220]. The basis of the electroporation technique relies on the transient generation of pores in the plasma membrane, to allow macromolecules to penetrate the cytoplasm and DNA to enter due to its negative charge [221]. Multiple electroporation systems have been described with respect to targeting different tissues in the developing chick, for example, the neural tube [222], the somites [223], and the eye [224]. In general, in ovo electroporation has been most commonly applied to chick embryos at early stages of development, younger than Hamburger and Hamilton stage 20 (HH20/∼E3.5). Therefore, an alternative to carrying out the DNA transfer in ovo for older embryos is to use shell-less culture techniques [225–229]. Such ex ovo methods have described using petri dishes [226], plastic cups [229], and drinking glasses [228]. These ex ovo methods provide additional accessibility that may be required in order to target a specific tissue at older stages of development. The use of this targeted technique may prove advantageous for investigating the molecular mechanisms involved in mechanoregulation, as it is possible to combine this technique with that of an altered mechanical environment.

4 COMPUTATIONAL TECHNIQUES IN MECHANOBIOLOGY

Computational techniques for probing research questions in the field of mechanobiology have developed alongside experimental investigations, as these techniques can both inform experimental design and glean new information from experimental observations. As computational power increases exponentially, these methods have become ever more sophisticated and enlightening. Indeed, many advances in mechanobiology have been spurred by computational investigation, shedding new light on problems ranging from the mechanical response, to loading of individual cells, to predicting tissue differentiation in response to loading.

While many experimental techniques exist to study mechanobiology, as outlined in the previous sections, almost all involve some sort of destructive interference with the tissue or cellular mechanical environment. Therefore, most mechanobiological problems represent excellent examples of Heisenberg's uncertainty principle, wherein it is effectively impossible to observe an intact in vivo mechanobiological environment without interfering with its native behavior. Examples of this include osteocytes in the bone [23], skeletal development in utero [230,231,231a,231b], cell migration in the intestinal epithelium [232], and growth of aortic aneurysms [233].

This section will outline a number of computational methods that have proved invaluable to the study of mechanobiology and will give a perspective on its future development as a field.

4.1 COMPUTATIONAL MODELING

Computational, or in silico, modeling comprises interdisciplinary methods that apply mathematics, physics, and computer science to replicate and analyze the behavior of complex systems through the use of computer simulation. By characterizing a system using numerous variables, the simulation can adjust these variables and predict the resulting effects on the system. In silico modeling of physical behaviors has developed from theoretical origins in the early 20th century into a powerful engineering tool to assess the mechanical behavior of physical structures; mechanical systems; and, more recently, biological processes. Rapid advances in computational power over the past two decades have brought computational modeling to the fore as a key tool to test prevailing theories or develop entirely new ones. The primary methods by which this is achieved are finite element (FE) method and finite volume method, whereby the system is broken down into a mesh of smaller, simpler regions, allowing modeling of solid or fluid behaviors, respectively. While FE modeling involves treating these elements like simple structures obeying physical laws, finite volume modeling calculates the change in flow of a fluid through the simple volume and into the next discrete volume. The standard physical equations solved in the elements or volumes are then assembled into a larger system of equations, allowing modeling and analysis of the entire problem [8]. The use of these techniques both complements and enhances the development of new and existing theoretical models in the field of mechanobiology. These techniques have been applied to a range of different tissues and diseases, a selection of which will be described in the following sections.

4.1.1 Computational fluid dynamics

Computational fluid dynamics (CFD) as a technique is readily applicable to the cardiovascular system, given its key role as a fluid transport system for the body. It has been applied for some time to investigate a wide range of vascular diseases, in disparate locations in the body. Since the early application of CFD methods to aneurysms in 1992 [234], they have developed rapidly to gain the confidence of clinicians as a strong diagnostic tool for predicting risk of rupture [235,236].

Similarly, the first application of CFD to coronary artery disease was published in 2000 [237] and has since been combined with significant advancements in medical imaging to develop realistic patient-specific models in 3D [238,239]. A recent and intriguing development is the study of mechanobiology of blood cells themselves using CFD [240], with multiple research groups simulating the interactions of crowded blood cell clusters in 3D [241–243]. Similar use of CFD in mechanobiology allows modeling the vitreous humor of the eye, predicting concentrations of shear stress on the chamber wall [244].

The other major mechanobiological application of CFD has been to predict flow of marrow or interstitial fluid within the bone. Early computational models were developed to characterize loading-induced fluid flow across whole bones [245]. Similar techniques were used to analyze an idealized lacunar-canalicular system, predicting abrupt changes in the drag forces within the canaliculi arising from changes in geometry or proximity to bone microporosity and haversian canals [246]. CFD techniques facilitated analysis of models of bone cells, in particular osteocytes, with idealized models predicting high shear stresses within the canaliculi [247]. More recently, CFD studies have demonstrated the importance of local geometry on fluid flow in the pericellular space, with geometries obtained from transmission electron microscopy (TEM) and ultrahigh-voltage electron microscopy (UHVEM) images suggested [248,249]. Additionally, numerical models have explored the effect of the pericellular matrix on flow through the canaliculus, investigating the permeability [250–252], fluid movement [253,254], and electrochemomechanical effects [254,255]. On a larger scale, shear stress within bone marrow under macroscopic loading has been characterized using CFD [256,257], predicting important mechanical stimuli for tissue engineering of the bone [258].

4.1.2 FE analysis

Given that the bone is a stiff, mechanically active, adaptive tissue, FE models have been employed for decades to investigate the biomechanics of the bone. Application of FE to orthopedic tissues began in 1972 [259] and initially was largely focused on either the design of prostheses or fundamental research into structural biomechanics [260]. More recently, FE has been used to determine adaptation of tissue structure in response to loading and mechanical stimuli at the tissue and cell levels under macroscale mechanical loading. Adaption is largely modeled through either tissue growth or tissue differentiation algorithms (reviewed in Ref. [8]), with these approaches being used to successfully model fracture healing [261], skeletal morphogenesis [230,262], and regeneration [263]. A range of mechanical stimuli at the tissue or cell level can be computed from models, predicting stress and strain [264,265], marrow shear stress [266–268], and even thermal stimuli [269] at the tissue and cellular scales. At the cellular level, first complete 3D idealized FE model of the bone cell environment predicted that strains in the lacunar walls are amplified by the local matrix geometry [270]. These findings were corroborated by recent FE studies applying accurate 3D geometries of osteocytes using scans from confocal

laser scanning microscopy and X-ray nanotomography, predicting that geometry alone can amplify strain transfer to the osteocyte in vivo [271,272]. FE models have also been applied to investigate mechanosensation of bone cells in vitro, allowing exploration of the stimulatory effects of cell morphology, focal adhesion density [273], and substrate material properties [274], as well as the translation of mechanical stimulation to the nucleus via the cytoskeleton [275].

The complex process of modeling of heart valve mechanics at the organ scale began as structural models, applying blood pressure as static loads [276–280]. Dynamic loading developed later and incorporated realistic geometries [281–283] and anisotropic [284] and nonlinear [285,286] material properties. At the tissue scale, research has concentrated on developing constitutive models to capture the mechanical behavior of heart valve tissue, with FE modeling recruited to implement these models (reviewed in detail elsewhere [287]). Modeling at the cell scale has developed recently and advanced rapidly, applying FE methods to either model the cell itself as a continuum [288,289] or characterize the structural behavior of the cytoskeleton [288,289].

Similar to the bone, cartilage is a mechanically responsive tissue for which FE analysis has provided many insights, including articular cartilage thickness distributions, skeletal morphology, and endochondral ossification patterns (reviewed in Ref. [290]). FE models have also been applied to investigate the expansion and growth of skin tissue, allowing the development of algorithms to predict mechanically controlled skin growth in health and disease [291–294]. Promising research into mechanics and mechanobiology in the vocal folds [295] and the vocal ligament [296] is also being carried out using FE analysis, demonstrating the wide breadth of research topics that benefit from these methods.

4.1.3 Multiscale and multiphysics modeling

While the various models outlined above focus on research questions confined to individual loading cases of a specific tissue structure or cell type, mechanobiology in vivo occurs across multiple scales, with translation of loading to cell and molecular levels followed by transduction into responses expressed at tissue and organ scales. Therefore, researchers across varying fields of study have recently applied multiscale modeling techniques to investigate this phenomenon.

In bone tissue, multiscale modeling techniques have been applied alongside periodic boundary conditions to determine that the strain experienced by osteocytes under the same macroscopic loading varies significantly and strongly depends on their location relative to microstructural porosities [297]. Furthermore, it was found that orientation of tissue structures such as lamellae can have a significant effect on strain experienced at the level of individual bone cells [297]). A similar multiscale FE approach has been applied to cells suspended in bone marrow, demonstrating the importance of cell-cell attachments for mechanosensation within the bone marrow under macroscopic bone loading [298].

Multiscale modeling has also been applied in more disparate cases, such as modeling fluid flow and matrix deformation in the liver, allowing optimization of

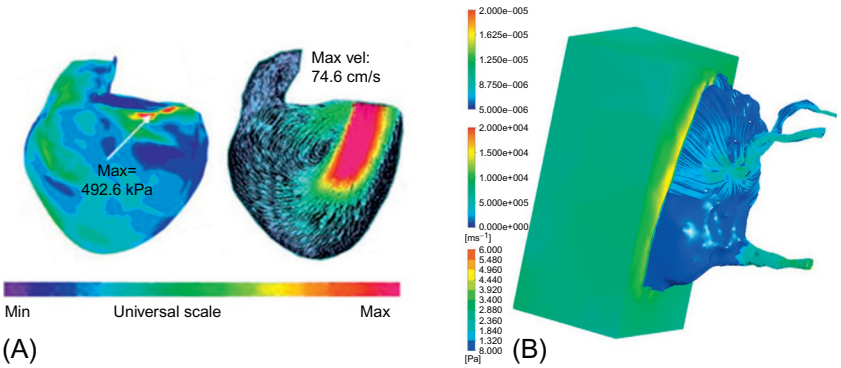

FIG. 7

Examples of fluid-structure interaction (FSI) models: (A) the contracting heart [301], showing stress distribution (left) and velocity profile (right); (B) an individual bone cell environment, with extracellular matrix strain, interstitial fluid velocity, and shear stress on the osteocyte surface shown [23].

perfusion conditions for tissue engineering [299]. In the study of morphogenesis, multiscale models are used both to investigate tissue-level effects in response to cellular- and molecular-scale events and to study cell arrangement in developing tissue [300].

As has been discussed, cells are exposed to various types of interrelated physical stimuli and therefore reside in a multiphysics environment. Multiphysics modeling represents a novel and developing array of methods that couple the effects of several physical phenomena in a single simulation or system of coupled simulations (see examples in Fig. 7). The type of multiphysics modeling most applicable to the study of mechanobiology is fluid-structure interaction (FSI) techniques, which couple classic CFD and FE modeling by relaying results between solvers in an iterative manner until a solution to both is converged upon. These new methods have been applied to models of in vitro systems, allowing determination of the mechanical stimulation applied to cells by experimental settings [302] and the stimulation experienced by individual cells at different locations in a tissue-engineering scaffold [303,304].

In the bone, FSI models have elucidated the function of the primary cilium as a mechanosensor on bone cells, determining the importance of cilia length [305]. Furthermore, FSI has been applied to the complex multiphysics environments within the bone, recently predicting that stimulatory magnitudes of shear stress result from macroscopic loading-induced fluid flow in accurate 3D models of osteocytes [23,306]. In an attempt to definitively compare these various mechanosensors, a comprehensive study of bone cell mechanosensation both in vitro and in vivo used FSI to predict that both integrin attachments and primary cilia are highly stimulated in vitro but that the primary cilia is less stimulated in vivo unless embedded in the surrounding matrix [307].

Multiscale techniques have been deployed to investigate in-stent restenosis alongside agent-based and cellular automata-based FE models of cell behavior [308–313], multiphysics modeling incorporating blood flow shear stress stimuli [314], and most recently mechanical/damage stimuli to individual cells [311], significantly advancing our understanding of this complex problem. Early advances were made in tying together mechanobiological stimuli across multiple scales and capturing multiphysics behavior in the aortic heart valve, with different forms of FSI simulations in this area developing over a decade of research (reviewed in detail elsewhere [315]). The use of these methods has shed new light on a range of different cardiovascular conditions, allowing analysis of transient, three-dimensional behavior over a range of length scales.

These multiscale and multiphysics models demonstrate the value of computational mechanobiology models for providing information on biophysical parameters that cannot be measured experimentally and the localized effects of multiple types of mechanosensors and complex patterns of physiological loading.

4.2 IMAGE ANALYSIS

One of the key problems in the study of mechanobiology is quantifying physical effects caused or experienced by cells, which is particularly challenging without directly interfering with them. While computational modeling attempts to recreate these effects, image analysis allows researchers to calculate the mechanics of mechanobiological behavior from experimental observations. These techniques can be developed in different manners and for various cells or tissues, with a selection of methods particularly useful in the field of mechanobiology discussed here.

4.2.1 Digital image correlation

Digital image correlation (DIC) is an optical technique that combines image registration and tracking methods for accurate 2D measurements of changes in images. Correlation theories for the measurement of alterations in data were first applied to digital images in 1975 [316]. These theories have been optimized in the recent years to apply to numerous applications [317], including confocal microscopy [318]. DIC is based upon the calculation of a correlation coefficient that is determined from pixel intensity array subsets on multiple corresponding images and extracting the deformation mapping function that relates the images. In this manner, the displacements of individual regions in an image are tracked over a series of images, with the resulting strain calculated.

DIC can thus be applied in mechanobiology to characterize strain at the tissue level or within individual cells under loading. The various tissues for which the technique has provided detailed strain maps and material properties include the skin [319,320]; the gallbladder [321]; the vasculature, such as the aorta [322–324]; the tympanic membrane of the ear [325]; and individual trabecular struts within bone [326]. DIC techniques have been recruited to diagnose cancer, as demonstrated by the detection of a basal cell carcinoma via strain mapping [327]. DIC can also

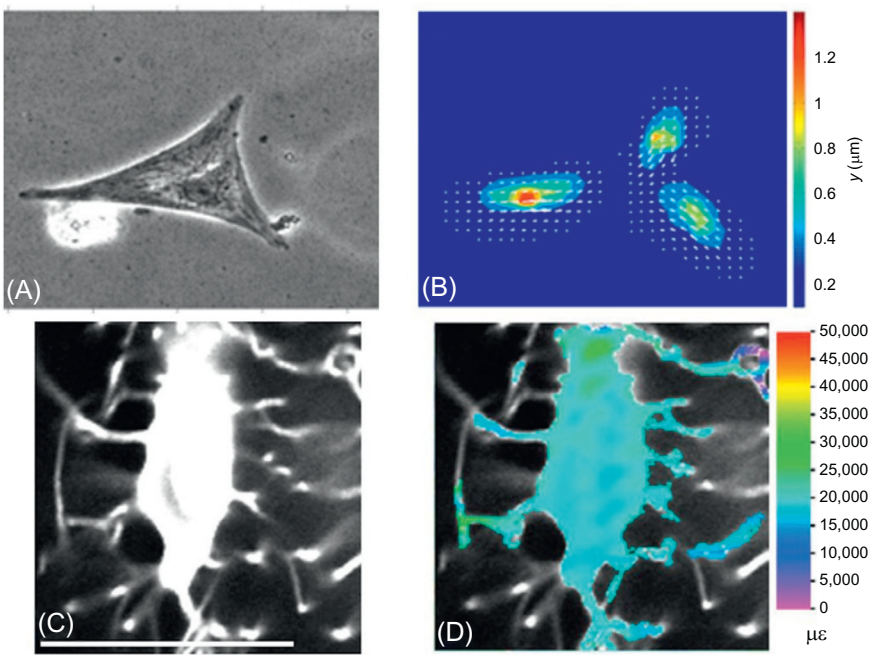

FIG. 8

Contour plots of cell mechanobiology developed using DIC: imaging of cell (A) contractility by (B) mapping substrate deformation [328] and imaging of (C) ex vivo osteocytes to generate contour plots of (D) cellular strains [329].

be applied at the scale of cells and can quantify the displacement field in a substrate under cell contraction [328] (Fig. 8A) or the velocity of cell migration [330]. A recent study applied this technique to osteocytes and osteoblasts in vivo, allowing cellular strains to be observed for the first time in bone tissue and providing direct evidence that loading of whole bones is amplified at the cell level [329] (Fig. 8B). DIC was also recently applied to analyze the beating of individual human cardiomyocytes, measuring both beating time and phases [331].

4.2.2 Particle image velocimetry

Developed over the past three decades, particle image velocimetry (PIV) has become a standard tool in experimental fluid mechanics. Given its ability to measure the instantaneous velocity field simultaneously at many points, it is possible to compute fluid vorticity and strain in rapidly evolving flows [332]. The technique has evolved from theoretical origins [333], with significant increases in computing power facilitating the development of digital PIV [334], while the advent and proliferation of standard digital cameras provided inputs perfectly suited to PIV [332].

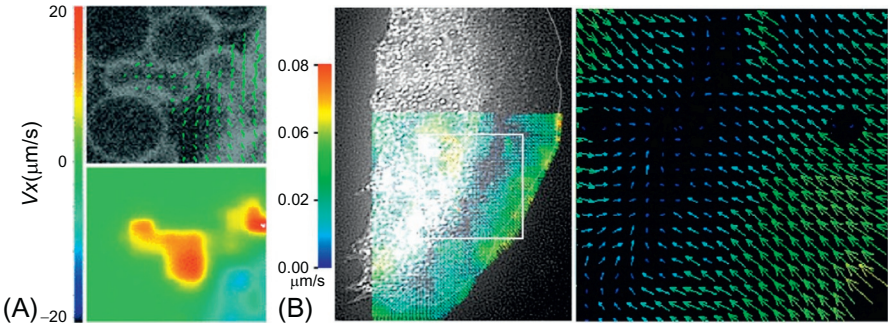

FIG. 9

The use of PIV allows imaging of (A) movement of individual red blood cells under flow [344] and (B) movement of the cytoskeleton within a cell [346].

PIV has been used extensively to investigate vascular biomechanics and mechanobiology, shedding light on the complex flow around heart valves and heart valve replacement devices [335–338]. Further development has facilitated the use of PIV to investigate flow inside bioreactors and scaffolds used for tissue engineering [339–341], including for the study of heart valve tissue mechanobiology [342]. Higher resolution capabilities have facilitated the investigation of cell level flow, including the dynamics of individual red blood cells [343]. Indeed, micro-PIV techniques are capable of capturing the flow around individual red blood cells [240,344]. In a fascinating application of the technology, it has recently been used at the cellular scale to calculate the shear stress affecting cell cytoskeletons [345] and to detect deformation of the cytoskeleton itself [346], as shown in Fig. 9. Finally, PIV has also been applied to capture the guidance of collective cell migration by substrate geometry [347] and the mechanical waves generated during the expansion of tissue, as occurs in both development [348] and cancer [349].

5 FUTURE PERSPECTIVES

Mechanobiology is a nascent field that, as is evident from the methods discussed, has benefitted from rapid advancements in molecular analysis, imaging, and computational techniques. Our understanding of mechanisms of mechanosensing and mechanotransduction is deepening, alongside growing recognition in many overlapping fields of the importance of mechanical effects in cell behavior, tissue development, and various diseases. In particular, the potential of mechanobiological tools to augment tissue engineering by replicating in vivo mechanical environments provides an important avenue of study. The precision through which experimental manipulation of mechanical stimuli has advanced, in addition to improvements in measurements of cell mechanics, provides opportunities to investigate mechanotransduction in ever greater detail. Furthermore, the power and sophistication of

computational tools have improved significantly and will likely spur further discoveries in the future. As engineering techniques become more intertwined with cellular and molecular analysis techniques, novel insights into the fundamental mechanisms by which cells appraise their mechanical environment will be gleaned. This will likely shed new light on the pathways by which cells transduce these stimuli into mechanical signals, presenting new therapeutic targets.

REFERENCES

[1] Arnoczky SP, Lavagnino M, Egerbacher M. The mechanobiological aetiopathogenesis of tendinopathy: is it the over-stimulation or the under-stimulation of tendon cells? Int J Exp Pathol 2007;88(4):217–26.
[2] Beaupre GS, Stevens SS, Carter DR. Mechanobiology in the development, maintenance, and degeneration of articular cartilage. J Rehabil Res Dev 2000;37(2):145–51.
[3] Chicurel ME, Chen CS, Ingber DE. Cellular control lies in the balance of forces. Curr Opin Cell Biol 1998;10(2):232–9.
[4] Eckes B, Krieg T. Regulation of connective tissue homeostasis in the skin by mechanical forces. Clin Exp Rheumatol 2004;22(3 Suppl. 33):S73–6.
[5] Grodzinsky AJ, Levenston ME, Jin M, Frank EH. Cartilage tissue remodeling in response to mechanical forces. Ann Rev Biomed Eng 2000;2:691–713.
[6] Ingber D. Mechanobiology and diseases of mechanotransduction. Ann Med 2003;35(8):564–77.
[7] Lammerding J, Kamm RD, Lee RT. Mechanotransduction in cardiac myocytes. Ann N Y Acad Sci 2004;1015:53–70.
[8] Giorgi M, Verbruggen SW, Lacroix D. In silico bone mechanobiology: modeling a multifaceted biological system. Wiley Interdiscip Rev Syst Biol Med 2016;8(6):485–505.
[9] Wang N, Tytell JD, Ingber DE. Mechanotransduction at a distance: mechanically coupling the extracellular matrix with the nucleus. Nat Rev Mol Cell Biol 2009;10(1):75.
[10] Eyckmans J, Boudou T, Yu X, Chen Christopher S. A hitchhiker's guide to mechanobiology. Dev Cell 2011;21(1):35–47.
[11] Harris A, Wild P, Stopak D. Silicone rubber substrata: a new wrinkle in the study of cell locomotion. Science (New York, NY) 1980;208(4440):177–9.
[12] Kung C. A possible unifying principle for mechanosensation. Nature 2005;436(7051):647–54.
[13] Civelekoglu-Scholey G, Scholey J. Mitotic force generators and chromosome segregation. Cell Mol Life Sci 2010;67(13):2231–50.
[14] Renkawitz J, Sixt M. Mechanisms of force generation and force transmission during interstitial leukocyte migration. EMBO Rep 2010;11(10):744–50.
[15] Robling AG, Hinant FM, Burr DB, Turner CH. Improved bone structure and strength after long-term mechanical loading is greatest if loading is separated into short bouts. J Bone Miner Res 2002;17(8):1545–54.
[16] Stamatialis DF, Papenburg BJ, Gironés M, Saiful S, Bettahalli SNM, Schmitmeier S, et al. Medical applications of membranes: drug delivery, artificial organs and tissue engineering. J Membr Sci 2008;308(1):1–34.
[17] Tondon A, Kaunas R. The direction of stretch-induced cell and stress fiber orientation depends on collagen matrix stress. PLoS One 2014;9(2):e89592.

[18] Castillo AB, Blundo JT, Chen JC, Lee KL, Yereddi NR, Jang E, et al. Focal adhesion kinase plays a role in osteoblast mechanotransduction in vitro but does not affect load-induced bone formation in vivo. PLoS One 2012;7(9):e43291.
[19] Merzouk S, Deuve JL, Dubois A, Navarro P, Avner P, Morey C. Lineage-specific regulation of imprinted X inactivation in extraembryonic endoderm stem cells. Epigenetics Chromatin 2014;7(1):11.
[20] Adachi T, Aonuma Y, S-i I, Tanaka M, Hojo M, Takano-Yamamoto T, et al. Osteocyte calcium signaling response to bone matrix deformation. J Biomech 2009;42(15):2507–12.
[21] Sugiyama T, Saxon LK, Zaman G, Moustafa A, Sunters A, Price JS, et al. Mechanical loading enhances the anabolic effects of intermittent parathyroid hormone (1–34) on trabecular and cortical bone in mice. Bone 2008;43(2):238–48.
[22] McNulty AL, Guilak F. Mechanobiology of the meniscus. J Biomech 2015;48(8):1469–78.
[23] Verbruggen SW, Vaughan TJ, McNamara LM. Fluid flow in the osteocyte mechanical environment: a fluid–structure interaction approach. Biomech Model Mechanobiol 2014;13(1):85–97.
[24] Ofek G, Athanasiou K. Micromechanical properties of chondrocytes and chondrons: relevance to articular cartilage tissue engineering. J Mech Mater Struct 2007;2(6):1059–86.
[25] Reynolds N. Experimental and computational investigation of the active force generation of cells subjected to static and dynamic loading (Doctoral dissertation). 2016.
[26] Rodriguez ML, McGarry PJ, Sniadecki NJ. Review on cell mechanics: experimental and modeling approaches. Appl Mech Rev 2013;65(6):060801.
[27] Hochmuth RM. Micropipette aspiration of living cells. J Biomech 2000;33(1):15–22.
[28] Ashkin A. Acceleration and trapping of particles by radiation pressure. Phys Rev Lett 1970;24(4):156.
[29] Ashkin A, Dziedzic JM. Optical trapping and manipulation of viruses and bacteria. Science (New York, NY) 1987;235:1517–21.
[30] Neuman KC, Nagy A. Single-molecule force spectroscopy: optical tweezers, magnetic tweezers and atomic force microscopy. Nat Methods 2008;5(6):491–505.
[31] Rotsch C, Jacobson K, Radmacher M. Dimensional and mechanical dynamics of active and stable edges in motile fibroblasts investigated by using atomic force microscopy. Proc Natl Acad Sci U S A 1999;96(3):921–6.
[32] Rotsch C, Radmacher M. Drug-induced changes of cytoskeletal structure and mechanics in fibroblasts: an atomic force microscopy study. Biophys J 2000;78(1):520–35.
[33] Stolz M, Raiteri R, Daniels A, VanLandingham MR, Baschong W, Aebi U. Dynamic elastic modulus of porcine articular cartilage determined at two different levels of tissue organization by indentation-type atomic force microscopy. Biophys J 2004;86(5):3269–83.
[34] Pelling AE, Dawson DW, Carreon DM, Christiansen JJ, Shen RR, Teitell MA, et al. Distinct contributions of microtubule subtypes to cell membrane shape and stability. Nanomed: Nanotechnol Biol Med 2007;3(1):43–52.
[35] Rico F, Roca-Cusachs P, Gavara N, Farré R, Rotger M, Navajas D. Probing mechanical properties of living cells by atomic force microscopy with blunted pyramidal cantilever tips. Phys Rev E 2005;72(2):021914.
[36] Mitchison J, Swann M. The mechanical properties of the cell surface. J Exp Biol 1954;31(3):461–72.

[37] Van Vliet K, Bao G, Suresh S. The biomechanics toolbox: experimental approaches for living cells and biomolecules. Acta Mater 2003;51(19):5881–905.
[38] Jones WR, Ping Ting-Beall H, Lee GM, Kelley SS, Hochmuth RM, Guilak F. Alterations in the Young's modulus and volumetric properties of chondrocytes isolated from normal and osteoarthritic human cartilage. J Biomech 1999;32(2):119–27.
[39] Sato M, Levesque MJ, Nerem RM. Micropipette aspiration of cultured bovine aortic endothelial cells exposed to shear stress. Arterioscl Thromb Vasc Biol 1987;7(3):276–86.
[40] Sato M, Ohshima N, Nerem RM. Viscoelastic properties of cultured porcine aortic endothelial cells exposed to shear stress. J Biomech 1996;29(4):461–7.
[41] Guilak F, Tedrow JR, Burgkart R. Viscoelastic properties of the cell nucleus. Biochem Biophys Res Commun 2000;269(3):781–6.
[42] Ribeiro AJS, Tottey S, Taylor RWE, Bise R, Kanade T, Badylak SF, et al. Mechanical characterization of adult stem cells from bone marrow and perivascular niches. J Biomech 2012;45(7):1280–7.
[43] Pravincumar P, Bader DL, Knight MM. Viscoelastic cell mechanics and actin remodelling are dependent on the rate of applied pressure. PLoS One 2012;7(9):e43938.
[44] Reynolds NH, Ronan W, Dowling EP, Owens P, McMeeking RM, McGarry JP. On the role of the actin cytoskeleton and nucleus in the biomechanical response of spread cells. Biomaterials 2014;35(13):4015–25.
[45] Reynolds NH, McGarry JP. Single cell active force generation under dynamic loading—part II: active modelling insights. Acta Biomater 2015;27:251–63.
[46] Deguchi S, Maeda K, Ohashi T, Sato M. Flow-induced hardening of endothelial nucleus as an intracellular stress-bearing organelle. J Biomech 2005;38(9):1751–9.
[46a] Kurth F, Eyer K, Franco-Obregón A, Dittrich PS. A new mechanobiological era: microfluidic pathways to apply and sense forces at the cellular level. Curr Opin Chem Biol 2012;16(3–4):400–8.
[46b] Bhatia SN, Ingber DE. Microfluidic organs-on-chips. Nat Biotechnol 2014;32(8):760.
[46c] Young EW. Cells, tissues, and organs on chips: challenges and opportunities for the cancer tumor microenvironment. Integrat Biol 2013;5(9):1096–109.
[46d] Hou HW, Lee WC, Leong MC, Sonam S, Vedula SRK, Lim CT. Microfluidics for applications in cell mechanics and mechanobiology. Cell Mol Bioeng 2011;4(4):591–602.
[47] Polacheck WJ, Chen CS. Measuring cell-generated forces: a guide to the available tools. Nat Methods 2016;13(5):415–23.
[48] Dembo M, Wang Y-L. Stresses at the cell-to-substrate interface during locomotion of fibroblasts. Biophys J 1999;76(4):2307–16.
[49] Hall MS, Long R, Feng X, Huang Y, Hui C-Y, Wu M. Toward single cell traction microscopy within 3D collagen matrices. Exp Cell Res 2013;319(16):2396–408.
[50] Style RW, Boltyanskiy R, German GK, Hyland C, MacMinn CW, Mertz AF, et al. Traction force microscopy in physics and biology. Soft Matter 2014;10(23):4047–55.
[51] Wang JH, Lin J-S. Cell traction force and measurement methods. Biomech Model Mechanobiol 2007;6(6):361–71.
[52] Balaban NQ, Schwarz US, Riveline D, Goichberg P, Tzur G, Sabanay I, et al. Force and focal adhesion assembly: a close relationship studied using elastic micropatterned substrates. Nat Cell Biol 2001;3(5):466.

[53] Beningo KA, Dembo M, Kaverina I, Small JV, Y-l W. Nascent focal adhesions are responsible for the generation of strong propulsive forces in migrating fibroblasts. J Cell Biol 2001;153(4):881–8.
[54] Dembo M, Oliver T, Ishihara A, Jacobson K. Imaging the traction stresses exerted by locomoting cells with the elastic substratum method. Biophys J 1996;70(4):2008–22.
[55] Jannat RA, Dembo M, Hammer DA. Traction forces of neutrophils migrating on compliant substrates. Biophys J 2011;101(3):575–84.
[56] Plotnikov SV, Pasapera AM, Sabass B, Waterman CM. Force fluctuations within focal adhesions mediate ECM-rigidity sensing to guide directed cell migration. Cell 2012;151(7):1513–27.
[57] Engler AJ, Sen S, Sweeney HL, Discher DE. Matrix elasticity directs stem cell lineage specification. Cell 2006;126(4):677–89.
[58] Kraning-Rush CM, Califano JP, Reinhart-King CA. Cellular traction stresses increase with increasing metastatic potential. PLoS One 2012;7(2):e32572.
[59] Lemmon CA, Sniadecki NJ, Ruiz SA, Tan JL, Romer LH, Chen CS. Shear force at the cell-matrix interface: enhanced analysis for microfabricated post array detectors. Mech Chem Biosyst 2005;2(1):1.
[60] Tan JL, Tien J, Pirone DM, Gray DS, Bhadriraju K, Chen CS. Cells lying on a bed of microneedles: an approach to isolate mechanical force. Proc Natl Acad Sci U S A 2003;100(4):1484–9.
[61] Du Roure O, Saez A, Buguin A, Austin RH, Chavrier P, Siberzan P, et al. Force mapping in epithelial cell migration. Proc Natl Acad Sci U S A 2005;102(7):2390–5.
[62] Sochol R, Higa A, Janairo R, Li S, Lin L. Effects of micropost spacing and stiffness on cell motility. Micro Nano Lett 2011;6(5):323–6.
[63] Ricart BG, Yang MT, Hunter CA, Chen CS, Hammer DA. Measuring traction forces of motile dendritic cells on micropost arrays. Biophys J 2011;101(11):2620–8.
[64] Rodriguez AG, Han SJ, Regnier M, Sniadecki NJ. Substrate stiffness increases twitch power of neonatal cardiomyocytes in correlation with changes in myofibril structure and intracellular calcium. Biophys J 2011;101(10):2455–64.
[65] Kural MH, Billiar KL. Mechanoregulation of valvular interstitial cell phenotype in the third dimension. Biomaterials 2014;35(4):1128–37.
[66] Fu J, Wang Y-K, Yang MT, Desai RA, Yu X, Liu Z, et al. Mechanical regulation of cell function with geometrically modulated elastomeric substrates. Nat Methods 2010;7(9):733–6.
[67] Liu Z, Tan JL, Cohen DM, Yang MT, Sniadecki NJ, Ruiz SA, et al. Mechanical tugging force regulates the size of cell–cell junctions. Proc Natl Acad Sci U S A 2010;107(22):9944–9.
[68] Ganz A, Lambert M, Saez A, Silberzan P, Buguin A, Mège RM, et al. Traction forces exerted through N-cadherin contacts. Biol Cell 2006;98(12):721–30.
[69] Pörtner R, Nagel-Heyer S, Goepfert C, Adamietz P, Meenen NM. Bioreactor design for tissue engineering. J Biosci Bioeng 2005;100(3):235–45.
[70] Darling EM, Athanasiou KA. Biomechanical strategies for articular cartilage regeneration. Ann Biomed Eng 2003;31(9):1114–24.
[71] Partap S, Plunkett N, O'brien F. Bioreactors in tissue engineering, In: Tissue engineering. InTechOpen; 2010, https://www.intechopen.com/books/tissue-engineering/bioreactors-in-tissue-engineering.

[72] Vunjak-Novakovic G, Obradovic B, Martin I, Bursac PM, Langer R, Freed LE. Dynamic cell seeding of polymer scaffolds for cartilage tissue engineering. Biotechnol Prog 1998;14(2):193–202.
[73] Bancroft GN, Sikavitsas VI, Mikos AG. Design of a flow perfusion bioreactor system for bone tissue-engineering applications. Tissue Eng 2003;9(3):549–54.
[74] Youngstrom DW, Barrett JG. Engineering tendon: scaffolds, bioreactors, and models of regeneration. Stem Cells Int 2015;2016:11 pages.
[75] Youngstrom DW, Rajpar I, Kaplan DL, Barrett JG. A bioreactor system for in vitro tendon differentiation and tendon tissue engineering. J Orthop Res 2015;33(6):911–8.
[76] Youngstrom DW, LaDow JE, Barrett JG. Tenogenesis of bone marrow-, adipose-, and tendon-derived stem cells in a dynamic bioreactor. Connect Tissue Res 2016;57(6):454–65.
[77] Burk J, Plenge A, Brehm W, Heller S, Pfeiffer B, Kasper C. Induction of tenogenic differentiation mediated by extracellular tendon matrix and short-term cyclic stretching. Stem Cells Int 2016;2016:11 pages.
[78] Mauck RL, Soltz MA, Wang CC, Wong DD, Chao P-HG, Valhmu WB, et al. Functional tissue engineering of articular cartilage through dynamic loading of chondrocyte-seeded agarose gels. J Biomech Eng 2000;122(3):252–60.
[79] Mauck RL, Nicoll SB, Seyhan SL, Ateshian GA, Hung CT. Synergistic action of growth factors and dynamic loading for articular cartilage tissue engineering. Tissue Eng 2003;9(4):597–611.
[80] Mauck RL, Seyhan SL, Ateshian GA, Hung CT. Influence of seeding density and dynamic deformational loading on the developing structure/function relationships of chondrocyte-seeded agarose hydrogels. Ann Biomed Eng 2002;30(8):1046–56.
[81] Mauck R, Byers B, Yuan X, Tuan R. Regulation of cartilaginous ECM gene transcription by chondrocytes and MSCs in 3D culture in response to dynamic loading. Biomech Model Mechanobiol 2007;6(1):113–25.
[82] McCoy RJ, O'Brien FJ. Influence of shear stress in perfusion bioreactor cultures for the development of three-dimensional bone tissue constructs: a review. Tissue Eng Part B: Rev 2010;16(6):587–601.
[83] Birmingham E, Kreipke T, Dolan E, Coughlin T, Owens P, McNamara LM, et al. Mechanical stimulation of bone marrow in situ induces bone formation in trabecular explants. Ann Biomed Eng 2015;43(4):1036–50.
[84] David V, Guignandon A, Martin A, Malaval L, Lafage-Proust M-H, Rattner A, et al. Ex vivo bone formation in bovine trabecular bone cultured in a dynamic 3D bioreactor is enhanced by compressive mechanical strain. Tissue Eng Part A 2008;14(1):117–26.
[85] Huang C, Charles Y, Hagar KL, Frost LE, Sun Y, Cheung HS. Effects of cyclic compressive loading on chondrogenesis of rabbit bone-marrow derived mesenchymal stem cells. Stem Cells 2004;22(3):313–23.
[86] Viens M, Chauvette G, Langelier È. A roadmap for the design of bioreactors in mechanobiological research and engineering of load-bearing tissues. J Med Devices 2011;5(4):041006–11.
[87] Henstock JR, El Haj AJ. Bioreactors. In: Mechanobiology: exploitation for medical benefit. Wiley Online Library; 2017. p. 275–96.
[88] Lanyon L, Hampson W, Goodship A, Shah J. Bone deformation recorded in vivo from strain gauges attached to the human tibial shaft. Acta Orthop Scand 1975;46(2):256–68.

[89] Usui T, Maki K, Toki Y, Shibasaki Y, Takanobu H, Takanishi A, et al. Measurement of mechanical strain on mandibular surface with mastication robot: influence of muscle loading direction and magnitude. Orthod Craniofac Res 2003;6(s1):163–7.
[90] Klein-Nulend J, Bacabac R, Bakker A. Mechanical loading and how it affects bone cells: the role of the osteocyte cytoskeleton in maintaining our skeleton. Eur Cell Mater 2012;24:278–91.
[91] Robling AG, Burr DB, Turner CH. Skeletal loading in animals. J Musculoskel Neuron Interact 2001;1(3):249–62.
[92] Turner C, Akhter M, Raab D, Kimmel D, Recker R. A noninvasive, in vivo model for studying strain adaptive bone modeling. Bone 1991;12(2):73–9.
[93] Torrance A, Mosley J, Suswillo R, Lanyon L. Noninvasive loading of the rat ulna in vivo induces a strain-related modeling response uncomplicated by trauma or periostal pressure. Calcif Tissue Int 1994;54(3):241–7.
[94] Robling AG, Burr DB, Turner CH. Recovery periods restore mechanosensitivity to dynamically loaded bone. J Exp Biol 2001;204(19):3389–99.
[95] Akhter M, Raab D, Turner C, Kimmel D, Recker R. Characterization of in vivo strain in the rat tibia during external application of a four-point bending load. J Biomech 1992;25 (10):1241–6.
[96] Akhter M, Cullen D, Pedersen E, Kimmel D, Recker R. Bone response to in vivo mechanical loading in two breeds of mice. Calcif Tissue Int 1998;63(5):442–9.
[97] Lee K, Maxwell A, Lanyon L. Validation of a technique for studying functional adaptation of the mouse ulna in response to mechanical loading. Bone 2002;31(3):407–12.
[98] Baumann AP, Aref MW, Turnbull TL, Robling AG, Niebur GL, Allen MR, et al. Development of an in vivo rabbit ulnar loading model. Bone 2015;75:55–61.
[99] van der Meulen MCH, Huiskes R. Why mechanobiology?: a survey article. J Biomech 2002;35(4):401–14.
[100] Rolfe R, Roddy K, Murphy P. Mechanical regulation of skeletal development. Curr Osteoporos Rep 2013;11(2):107–16.
[101] Stern CD. The chick; a great model system becomes even greater. Dev Cell 2005;8 (1):9–17.
[102] King ED, Munger BL. Myotome and early neurogenesis in chick embryos. Anat Rec 1990;228(2):191–210.
[103] Hamburger V. Some aspects of the embryology of behavior. Q Rev Biol 1963;38:342–65.
[104] Nowlan NC, Prendergast PJ, Murphy P. Identification of mechanosensitive genes during embryonic bone formation. PLoS Comput Biol 2008;4(12):e1000250.
[105] Osborne AC, Lamb KJ, Lewthwaite JC, Dowthwaite GP, Pitsillides AA. Short-term rigid and flaccid paralyses diminish growth of embryonic chick limbs and abrogate joint cavity formation but differentially preserve pre-cavitated joints. J Musculoskelet Neuronal Interact 2002;2(5):448–56.
[106] Rolfe RA, Bezer JH, Kim T, Zaidon AZ, Oyen ML, Iatridis JC, et al. Abnormal fetal muscle forces result in defects in spinal curvature and alterations in vertebral segmentation and shape. J Orthop Res 2017;35(10):2135–44.
[107] Murray PD, Drachman DB. The role of movement in the development of joints and related structures: the head and neck in the chick embryo. J Embryol Exp Morphol 1969;22(3):349–71.

[108] Nowlan NC, Chandaria V, Sharpe J. Immobilized chicks as a model system for early-onset developmental dysplasia of the hip. J Orthop Res 2014;32(6):777–85.
[109] Persson M. The role of movements in the development of sutural and diarthrodial joints tested by long-term paralysis of chick embryos. J Anat 1983;137(Pt 3):591–9.
[110] Roddy KA, Prendergast PJ, Murphy P. Mechanical influences on morphogenesis of the knee joint revealed through morphological, molecular and computational analysis of immobilised embryos. PLoS One 2011;6(2):e17526.
[111] Suzue T. Movements of mouse fetuses in early stages of neural development studied in vitro. Neurosci Lett 1996;218(2):131–4.
[112] Rudnicki MA, Schnegelsberg PN, Stead RH, Braun T, Arnold HH, Jaenisch R. MyoD or Myf-5 is required for the formation of skeletal muscle. Cell 1993;75(7):1351–9.
[113] Pai AC. Developmental genetics of a lethal mutation, muscular dysgenesis (mdg), in the mouse. II. Developmental analysis. Dev Biol 1965;11:93–109.
[114] Franz T, Kothary R, Surani MA, Halata Z, Grim M. The Splotch mutation interferes with muscle development in the limbs. Anat Embryol (Berl) 1993;187(2):153–60.
[115] Tajbakhsh S, Rocancourt D, Cossu G, Buckingham M. Redefining the genetic hierarchies controlling skeletal myogenesis: Pax-3 and Myf-5 act upstream of MyoD. Cell 1997;89(1):127–38.
[116] Franz T. The Splotch (Sp1H) and Splotch-delayed (Spd) alleles: differential phenotypic effects on neural crest and limb musculature. Anat Embryol (Berl) 1993;187(4):371–7.
[117] Vogan KJ, Epstein DJ, Trasler DG, Gros P. The splotch-delayed (Spd) mouse mutant carries a point mutation within the paired box of the Pax-3 gene. Genomics 1993;17(2):364–9.
[118] Kassar-Duchossoy L, Gayraud-Morel B, Gomes D, Rocancourt D, Buckingham M, Shinin V, et al. Mrf4 determines skeletal muscle identity in Myf5:Myod double-mutant mice. Nature 2004;431(7007):466–71.
[119] Kablar B, Krastel K, Tajbakhsh S, Rudnicki MA. Myf5 and MyoD activation define independent myogenic compartments during embryonic development. Dev Biol 2003;258(2):307–18.
[120] Grifone R, Demignon J, Houbron C, Souil E, Niro C, Seller MJ, et al. Six1 and Six4 homeoproteins are required for Pax3 and Mrf expression during myogenesis in the mouse embryo. Development 2005;132(9):2235–49.
[121] Nowlan NC, Bourdon C, Dumas G, Tajbakhsh S, Prendergast PJ, Murphy P. Developing bones are differentially affected by compromised skeletal muscle formation. Bone 2010;46(5):1275–85.
[122] Hammond CL, Moro E. Using transgenic reporters to visualize bone and cartilage signaling during development in vivo. Front Endocrinol 2012;3:91.
[123] Brunt LH, Norton JL, Bright JA, Rayfield EJ, Hammond CL. Finite element modelling predicts changes in joint shape and cell behaviour due to loss of muscle strain in jaw development. J Biomech 2015;48(12):3112–22.
[124] Shwartz Y, Farkas Z, Stern T, Aszodi A, Zelzer E. Muscle contraction controls skeletal morphogenesis through regulation of chondrocyte convergent extension. Dev Biol 2012;370(1):154–63.
[125] Brunt LH, Skinner RE, Roddy KA, Araujo NM, Rayfield EJ, Hammond CL. Differential effects of altered patterns of movement and strain on joint cell behaviour and skeletal morphogenesis. Osteoarthritis Cartilage 2016;24(11):1940–50.
[126] Brunt LH, Begg K, Kague E, Cross S, Hammond CL. Wnt signalling controls the response to mechanical loading during Zebrafish joint development. Development 2017;144(15):2798–809.

[127] Shimomura O, Johnson FH, Saiga Y. Extraction, purification and properties of aequorin, a bioluminescent protein from the luminous hydromedusan, aequorea. J Cell Comp Physiol 1962;59(3):223–39.
[128] Lippincott-Schwartz J, Patterson GH. Development and use of fluorescent protein markers in living cells. Science (New York, NY) 2003;300(5616):87–91.
[129] Wang Y, Shyy JY, Chien S. Fluorescence proteins, live-cell imaging, and mechanobiology: seeing is believing. Annu Rev Biomed Eng 2008;10:1–38.
[130] Tsien RY. The green fluorescent protein. USA: Annual Reviews; 1998.
[131] Rowat A, Lammerding J, Ipsen JH. Mechanical properties of the cell nucleus and the effect of emerin deficiency. Biophys J 2006;91(12):4649–64.
[132] Wang N, Naruse K, Stamenović D, Fredberg JJ, Mijailovich SM, Tolić-Nørrelykke IM, et al. Mechanical behavior in living cells consistent with the tensegrity model. Proc Natl Acad Sci U S A 2001;98(14):7765–70.
[133] Hu S, Chen J, Fabry B, Numaguchi Y, Gouldstone A, Ingber DE, et al. Intracellular stress tomography reveals stress focusing and structural anisotropy in cytoskeleton of living cells. Am J Physiol Cell Physiol 2003;285(5):C1082–90.
[134] Kumar S, Maxwell IZ, Heisterkamp A, Polte TR, Lele TP, Salanga M, et al. Viscoelastic retraction of single living stress fibers and its impact on cell shape, cytoskeletal organization, and extracellular matrix mechanics. Biophys J 2006;90(10):3762–73.
[135] Hu K, Ji L, Applegate KT, Danuser G, Waterman-Storer CM. Differential transmission of actin motion within focal adhesions. Science (New York, NY) 2007;315 (5808):111–5.
[136] Lele TP, Pendse J, Kumar S, Salanga M, Karavitis J, Ingber DE. Mechanical forces alter zyxin unbinding kinetics within focal adhesions of living cells. J Cell Physiol 2006;207 (1):187–94.
[137] Kirchner J, Kam Z, Tzur G, Bershadsky AD, Geiger B. Live-cell monitoring of tyrosine phosphorylation in focal adhesions following microtubule disruption. J Cell Sci 2003;116(6):975–86.
[138] Giannone G, Dubin-Thaler BJ, Rossier O, Cai Y, Chaga O, Jiang G, et al. Lamellipodial actin mechanically links myosin activity with adhesion-site formation. Cell 2007;128 (3):561–75.
[139] Gupton SL, Waterman-Storer CM. Spatiotemporal feedback between actomyosin and focal-adhesion systems optimizes rapid cell migration. Cell 2006;125(7):1361–74.
[140] Zamir E, Katz M, Posen Y, Erez N, Yamada KM, Katz B-Z, et al. Dynamics and segregation of cell-matrix adhesions in cultured fibroblasts. Nat Cell Biol 2000; 2(4):191.
[141] Galbraith CG, Yamada KM, Sheetz MP. The relationship between force and focal complex development. J Cell Biol 2002;159(4):695–705.
[142] Mack PJ, Kaazempur-Mofrad MR, Karcher H, Lee RT, Kamm RD. Force-induced focal adhesion translocation: effects of force amplitude and frequency. Am J Physiol Cell Physiol 2004;287(4):C954–62.
[143] Sawada Y, Tamada M, Dubin-Thaler BJ, Cherniavskaya O, Sakai R, Tanaka S, et al. Force sensing by mechanical extension of the Src family kinase substrate p130Cas. Cell 2006;127(5):1015–26.
[144] Guo W-h, Y-l W. Retrograde fluxes of focal adhesion proteins in response to cell migration and mechanical signals. Mol Biol Cell 2007;18(11):4519–27.
[145] Wang Y, Chang J, Li Y-C, Li Y-S, Shyy JY-J, Chien S. Shear stress and VEGF activate IKK via the Flk-1/Cbl/Akt signaling pathway. Am J Physiol Heart Circ Physiol 2004;286(2):H685–92.

[146] Ji JY, Jing H, Diamond SL. Shear stress causes nuclear localization of endothelial glucocorticoid receptor and expression from the GRE promoter. Circ Res 2003;92(3):279–85.
[147] Ganguli A, Persson L, Palmer IR, Evans I, Yang L, Smallwood R, et al. Distinct NF-κB regulation by shear stress through Ras-dependent IκBα oscillations. Circ Res 2005;96(6):626–34.
[148] Oancea E, Wolfe JT, Clapham DE. Functional TRPM7 channels accumulate at the plasma membrane in response to fluid flow. Circ Res 2006;98(2):245–53.
[149] Ettinger A, Wittmann T. Fluorescence live cell imaging. Methods Cell Biol 2014;123:77–94.
[150] Chachisvilis M, Zhang Y-L, Frangos JA. G protein-coupled receptors sense fluid shear stress in endothelial cells. Proc Natl Acad Sci U S A 2006;103(42):15463–8.
[151] Zhao M, Wan X, Li Y, Zhou W, Peng L. Multiplexed 3D FRET imaging in deep tissue of live embryos. Sci Rep 2015;5:13991.
[152] Gomes P, Malfait M, Himpens B, Vereecke J. Intercellular Ca2+-transient propagation in normal and high glucose solutions in rat retinal epithelial (RPE-J) cells during mechanical stimulation. Cell Calcium 2003;34(2):185–92.
[153] Himpens B, Stalmans P, Gomez P, Malfait M, Vereecke J. Intra-and intercellular Ca2+ signaling in retinal pigment epithelial cells during mechanical stimulation. FASEB J 1999;13(9001):S63–8.
[154] Wolf K, Friedl P. Molecular mechanisms of cancer cell invasion and plasticity. Br J Dermatol 2006;154(s1):11–5.
[155] Pedersen JA, Swartz MA. Mechanobiology in the third dimension. Ann Biomed Eng 2005;33(11):1469–90.
[156] Even-Ram S, Yamada KM. Cell migration in 3D matrix. Curr Opin Cell Biol 2005;17(5):524–32.
[157] Goggin PM, Zygalakis KC, Oreffo RO, Schneider P. High-resolution 3D imaging of osteocytes and computational modelling in mechanobiology: insights on bone development, ageing, health and disease. Eur Cell Mater 2016;31:264–95.
[158] Periasamy A, Skoglund P, Noakes C, Keller R. An evaluation of two-photon excitation versus confocal and digital deconvolution fluorescence microscopy imaging in *Xenopus morphogenesis*. Microsc Res Tech 1999;47(3):172–81.
[159] Shotton DM. Confocal scanning optical microscopy and its applications for biological specimens. J Cell Sci 1989;94(2):175–206.
[160] Denk W, Strickler JH, Webb WW. Two-photon laser scanning fluorescence microscopy. Science (New York, NY) 1990;248(4951):73–6.
[161] Helmchen F, Denk W. Deep tissue two-photon microscopy. Nat Methods 2005;2(12):932–40.
[162] Rubart M. Two-photon microscopy of cells and tissue. Circ Res 2004;95(12):1154–66.
[163] Koutalos Y. Intracellular spreading of second messengers. J Physiol 1999;519(3):629.
[164] Weiss S. Fluorescence spectroscopy of single biomolecules. Science (New York, NY) 1999;283(5408):1676–83.
[165] Centonze VE, White JG. Multiphoton excitation provides optical sections from deeper within scattering specimens than confocal imaging. Biophys J 1998;75(4):2015–24.
[165a] Curley CJ, Dolan EB, Cavanagh B, O'Sullivan J, Duffy GP, Murphy BP. An in vitro investigation to assess procedure parameters for injecting therapeutic hydrogels into the myocardium. J Biomed Mater Res B 2017;105(8):2618–29.

[165b] Payne C, Dolan EB, O'Sullivan J, Cryan SA, Kelly H. A methylcellulose and collagen based temperature responsive hydrogel promotes encapsulated stem cell viability and proliferation in vitro. Drug Deliv Translat Res 2017;7:132.
[166] Steward AJ, Kelly DJ. Mechanical regulation of mesenchymal stem cell differentiation. J Anat 2014;.
[167] Potter CM, Lao KH, Zeng L, Xu Q. Role of biomechanical forces in stem cell vascular lineage differentiation. Arterioscler Thromb Vasc Biol 2014;34(10):2184–90.
[168] Pirrung MC, Southern EM. The genesis of microarrays. Biochem Mol Biol Educ 2014;42(2):106–13.
[169] Patel MJ, Liu W, Sykes MC, Ward NE, Risin SA, Risin D, et al. Identification of mechanosensitive genes in osteoblasts by comparative microarray studies using the rotating wall vessel and the random positioning machine. J Cell Biochem 2007;101 (3):587–99.
[170] Scholtes S, Kramer E, Weisser M, Roth W, Luginbuhl R, Grossner T, et al. Global chondrocyte gene expression after a single anabolic loading period: time evolution and re-inducibility of mechano-responses. J Cell Physiol 2018;233(1):699–711.
[171] Bougault C, Aubert-Foucher E, Paumier A, Perrier-Groult E, Huot L, Hot D, et al. Dynamic compression of chondrocyte-agarose constructs reveals new candidate mechanosensitive genes. PLoS One 2012;7(5):e36964.
[172] Sironen RK, Karjalainen HM, Elo MA, Kaarniranta K, Torronen K, Takigawa M, et al. cDNA array reveals mechanosensitive genes in chondrocytic cells under hydrostatic pressure. Biochim Biophys Acta 2002;1591(1–3):45–54.
[173] Rolfe RA, Nowlan NC, Kenny EM, Cormican P, Morris DW, Prendergast PJ, et al. Identification of mechanosensitive genes during skeletal development: alteration of genes associated with cytoskeletal rearrangement and cell signalling pathways. BMC Genomics 2014;15(1):48.
[174] Mortazavi A, Williams BA, McCue K, Schaeffer L, Wold B. Mapping and quantifying mammalian transcriptomes by RNA-Seq. Nat Methods 2008;5(7):621–8.
[175] Ozsolak F. Third-generation sequencing techniques and applications to drug discovery. Expert Opin Drug Discov 2012;7(3):231–43.
[176] Wilhelm BT, Landry JR. RNA-Seq-quantitative measurement of expression through massively parallel RNA-sequencing. Methods 2009;48(3):249–57.
[177] Bottomly D, Walter NA, Hunter JE, Darakjian P, Kawane S, Buck KJ, et al. Evaluating gene expression in C57BL/6J and DBA/2J mouse striatum using RNA-Seq and microarrays. PLoS One 2011;6(3):e17820.
[178] Lahiry P, Lee LJ, Frey BJ, Rupar CA, Siu VM, Blencowe BJ, et al. Transcriptional profiling of endocrine cerebro-osteodysplasia using microarray and next-generation sequencing. PLoS One 2011;6(9):e25400.
[179] Marioni JC, Mason CE, Mane SM, Stephens M, Gilad Y. RNA-seq: an assessment of technical reproducibility and comparison with gene expression arrays. Genome Res 2008;18(9):1509–17.
[180] Wang Z, Gerstein M, Snyder M. RNA-Seq: a revolutionary tool for transcriptomics. Nat Rev Genet 2009;10(1):57–63.
[181] Le Bleu HK, Kamal FA, Kelly M, Ketz JP, Zuscik MJ, Elbarbary RA. Extraction of high-quality RNA from human articular cartilage. Anal Biochem 2017;518:134–8.
[182] Poirion OB, Zhu X, Ching T, Garmire L. Single-cell transcriptomics bioinformatics and computational challenges. Front Genet 2016;7:163.

[183] Wu AR, Neff NF, Kalisky T, Dalerba P, Treutlein B, Rothenberg ME, et al. Quantitative assessment of single-cell RNA-sequencing methods. Nat Methods 2014;11(1):41–6.
[184] Livak KJ, Schmittgen TD. Analysis of relative gene expression data using real-time quantitative PCR and the 2(-Delta Delta C(T)) method. Methods 2001;25(4):402–8.
[185] Saha A, Rolfe R, Carroll S, Kelly DJ, Murphy P. Chondrogenesis of embryonic limb bud cells in micromass culture progresses rapidly to hypertrophy and is modulated by hydrostatic pressure. Cell Tissue Res 2016;.
[186] Juhasz T, Matta C, Somogyi C, Katona E, Takacs R, Soha RF, et al. Mechanical loading stimulates chondrogenesis via the PKA/CREB-Sox9 and PP2A pathways in chicken micromass cultures. Cell Signal 2014;26(3):468–82.
[187] Vinardell T, Rolfe RA, Buckley CT, Meyer EG, Ahearne M, Murphy P, et al. Hydrostatic pressure acts to stabilise a chondrogenic phenotype in porcine joint tissue derived stem cells. Eur Cell Mater 2012;23:121–32 [discussion 33-4].
[188] Derderian CA, Bastidas N, Lerman OZ, Bhatt KA, Lin S-E, Voss J, et al. Mechanical strain alters gene expression in an in vitro model of hypertrophic scarring. Ann Plast Surg 2005;55(1):69–75.
[189] Overby DR, Zhou EH, Vargas-Pinto R, Pedrigi RM, Fuchshofer R, Braakman ST, et al. Altered mechanobiology of Schlemm's canal endothelial cells in glaucoma. Proc Natl Acad Sci U S A 2014;111(38):13876–81.
[190] Dolan EB, Haugh MG, Voisin MC, Tallon D, McNamara LM. Thermally induced osteocyte damage initiates a remodelling signaling cascade. PLoS One 2015;10(3):e0119652.
[191] Dolan EB, Tallon D, Cheung W-Y, Schaffler MB, Kennedy OD, McNamara LM. Thermally induced osteocyte damage initiates pro-osteoclastogenic gene expression in vivo. J R Soc Interface 2016;13(119):20160337.
[192] Pardue ML, Gall JG. Molecular hybridization of radioactive DNA to the DNA of cytological preparations. Proc Natl Acad Sci U S A 1969;64(2):600–4.
[193] Jensen E. Technical review: in situ hybridization. Anat Rec (Hoboken, NJ) 2014;297(8):1349–53.
[194] Kahn J, Shwartz Y, Blitz E, Krief S, Sharir A, Breitel DA, et al. Muscle contraction is necessary to maintain joint progenitor cell fate. Dev Cell 2009;16(5):734–43.
[195] Barreto S, Gonzalez-Vazquez A, Cameron AR, Cavanagh B, Murray DJ, O'Brien FJ. Identification of the mechanisms by which age alters the mechanosensitivity of mesenchymal stromal cells on substrates of differing stiffness: Implications for osteogenesis and angiogenesis. Acta Biomater 2017;53:59–69.
[196] Nowlan NC, Dumas G, Tajbakhsh S, Prendergast PJ, Murphy P. Biophysical stimuli induced by passive movements compensate for lack of skeletal muscle during embryonic skeletogenesis. Biomech Model Mechanobiol 2012;11(1-2):207–19.
[197] Singh PN, Ray A, Azad K, Bandyopadhyay A. A comprehensive mRNA expression analysis of developing chicken articular cartilage. Gene Expr Patterns 2016;20(1):22–31.
[198] Kavanagh E, Church VL, Osborne AC, Lamb KJ, Archer CW, Francis-West PH, et al. Differential regulation of GDF-5 and FGF-2/4 by immobilisation in ovo exposes distinct roles in joint formation. Dev Dyn 2006;235(3):826–34.
[199] Roddy KA, Kelly GM, van Es MH, Murphy P, Prendergast PJ. Dynamic patterns of mechanical stimulation co-localise with growth and cell proliferation during morphogenesis in the avian embryonic knee joint. J Biomech 2011;.
[200] Wasik AA, Schiller HB. Functional proteomics of cellular mechanosensing mechanisms. Semin Cell Dev Biol 2017;71:118–28.

[201] Mahmood T, Yang PC. Western blot: technique, theory, and trouble shooting. N Am J Med Sci 2012;4(9):429–34.
[202] Carroll SF, Buckley CT, Kelly DJ. Cyclic hydrostatic pressure promotes a stable cartilage phenotype and enhances the functional development of cartilaginous grafts engineered using multipotent stromal cells isolated from bone marrow and infrapatellar fat pad. J Biomech 2014;47(9):2115–21.
[203] Thorpe SD, Buckley CT, Vinardell T, O'Brien FJ, Campbell VA, Kelly DJ. The response of bone marrow-derived mesenchymal stem cells to dynamic compression following TGF-beta3 induced chondrogenic differentiation. Ann Biomed Eng 2010;38 (9):2896–909.
[204] Coughlin TR, Schiavi J, Alyssa Varsanik M, Voisin M, Birmingham E, Haugh MG, et al. Primary cilia expression in bone marrow in response to mechanical stimulation in explant bioreactor culture. Eur Cell Mater 2016;32:111–22.
[205] Espinha LC, Hoey DA, Fernandes PR, Rodrigues HC, Jacobs CR. Oscillatory fluid flow influences primary cilia and microtubule mechanics. Cytoskeleton (Hoboken, NJ) 2014;71(7):435–45.
[206] Upadhyay VS, Muntean BS, Kathem SH, Hwang JJ, AbouAlaiwi WA, Nauli SM. Roles of dopamine receptor on chemosensory and mechanosensory primary cilia in renal epithelial cells. Front Physiol 2014;5:72–8.
[207] Dupont S, Morsut L, Aragona M, Enzo E, Giulitti S, Cordenonsi M, et al. Role of YAP/TAZ in mechanotransduction. Nature 2011;474(7350):179–83.
[208] Engvall E, Perlmann P. Enzyme-linked immunosorbent assay (ELISA) quantitative assay of immunoglobulin G. Immunochemistry 1971;8(9):871–4.
[209] Kragstrup TW, Vorup-Jensen T, Deleuran B, Hvid M. A simple set of validation steps identifies and removes false results in a sandwich enzyme-linked immunosorbent assay caused by anti-animal IgG antibodies in plasma from arthritis patients. Springerplus 2013;2(1):263.
[210] Nagatomi J. Mechanobiology handbook. Florida, United States: CRC Press; 2011.
[211] Hartman RA, Bell KM, Debski RE, Kang JD, Sowa GA. Novel ex-vivo mechanobiological intervertebral disc culture system. J Biomech 2012;45(2):382–5.
[212] Merryman WD, Youn I, Lukoff HD, Krueger PM, Guilak F, Hopkins RA, et al. Correlation between heart valve interstitial cell stiffness and transvalvular pressure: implications for collagen biosynthesis. Am J Physiol Heart Circ Physiol 2006;290(1): H224–31.
[213] Polacheck WJ, Li R, Uzel SG, Kamm RD. Microfluidic platforms for mechanobiology. Lab Chip 2013;13(12):2252–67.
[214] Mei Y, Wang Y, Chen H, Sun ZS, Ju XD. Recent progress in CRISPR/Cas9 technology. J Genet Genomics 2016;43(2):63–75.
[215] Wade M. High-throughput silencing using the CRISPR-Cas9 system: a review of the benefits and challenges. J Biomol Screen 2015;20(8):1027–39.
[216] Jinek M, Chylinski K, Fonfara I, Hauer M, Doudna JA, Charpentier E. A programmable dual-RNA-guided DNA endonuclease in adaptive bacterial immunity. Science (New York, NY) 2012;337(6096):816–21.
[217] Suzuki H, Ito Y, Shinohara M, Yamashita S, Ichinose S, Kishida A, et al. Gene targeting of the transcription factor Mohawk in rats causes heterotopic ossification of Achilles tendon via failed tenogenesis. Proc Natl Acad Sci U S A 2016;113(28): 7840–5.
[218] Gordon CT, Rodda FA, Farlie PG. The RCAS retroviral expression system in the study of skeletal development. Dev Dyn 2009;238(4):797–811.

[219] Muramatsu T, Mizutani Y, Ohmori Y, Okumura J. Comparison of three nonviral transfection methods for foreign gene expression in early chicken embryos in ovo. Biochem Biophys Res Commun 1997;230(2):376–80.
[220] Muramatsu TMY, Okumura J. Live detection of the firefly luciferase gene expression by bioluminescence in incubating chicken embryos. Anim Sci Technol (Jpn) 1996;67 (10):906–9.
[221] Potter H, Weir L, Leder P. Enhancer-dependent expression of human kappa immunoglobulin genes introduced into mouse pre-B lymphocytes by electroporation. Proc Natl Acad Sci U S A 1984;81(22):7161–5.
[222] Miller-Delaney SF, Lieberam I, Murphy P, Mitchell KJ. Plxdc2 is a mitogen for neural progenitors. PLoS One 2011;6(1):e14565.
[223] Scaal M, Gros J, Lesbros C, Marcelle C. In ovo electroporation of avian somites. Dev Dyn 2004;229(3):643–50.
[224] Durand C, Bangs F, Signolet J, Decker E, Tickle C, Rappold G. Enhancer elements upstream of the SHOX gene are active in the developing limb. Eur J Hum Genet 2010;18(5):527–32.
[225] Datar S, Bhonde RR. Shell-less chick embryo culture as an alternative in vitro model to investigate glucose-induced malformations in mammalian embryos. Rev Diabet Stud 2005;2(4):221–7.
[226] El-Ghali N, Rabadi M, Ezin AM, De Bellard ME. New methods for chicken embryo manipulations. Microsc Res Tech 2010;73(1):58–66.
[227] Luo J, Yan X, Lin J, Rolfs A. Gene transfer into older chicken embryos by ex ovo electroporation. J Vis Exp 2012;(65):4078–81.
[228] Schomann T, Qunneis F, Widera D, Kaltschmidt C, Kaltschmidt B. Improved method for ex ovo-cultivation of developing chicken embryos for human stem cell xenografts. Stem Cells Int 2013;2013:960958.
[229] Yalcin HC, Shekhar A, Rane AA, Butcher JT. An ex-ovo chicken embryo culture system suitable for imaging and microsurgery applications. J Vis Exp 2010;(44):2154–8.
[230] Giorgi M, Carriero A, Shefelbine SJ, Nowlan NC. Effects of normal and abnormal loading conditions on morphogenesis of the prenatal hip joint: application to hip dysplasia. J Biomech 2015;48(12):3390–7.
[231] Verbruggen SW, Loo JHW, Hayat TTA, Hajnal JV, Rutherford MA, Phillips ATM, et al. Modeling the biomechanics of fetal movements. Biomech Model Mechanobiol 2016;15(4):995–1004.
[231a] Verbruggen SW, Kainz B, Shelmerdine SC, Hajnal JV, Rutherford MA, Arthurs OJ, Phillips AT, Nowlan NC. Stresses and strains on the human fetal skeleton during development. J R Soc Interface 2018;15(138):20170593.
[231b] Verbruggen SW, Oyen ML, Phillips AT, Nowlan NC. Function and failure of the fetal membrane: modelling the mechanics of the chorion and amnion. PLoS ONE 2017;12 (3):e0171588.
[232] Wong SY, Chiam K-H, Lim CT, Matsudaira P. Computational model of cell positioning: directed and collective migration in the intestinal crypt epithelium. J R Soc Interface 2010;7(Suppl. 3):S351–63.
[233] Humphrey JD, Holzapfel GA. Mechanics, mechanobiology, and modeling of human abdominal aorta and aneurysms. J Biomech 2012;45(5):805–14.
[234] Gonzalez CF, Cho YI, Ortega HV, Moret J. Intracranial aneurysms: flow analysis of their origin and progression. Am J Neuroradiol 1992;13(1):181–8.
[235] Robertson AM, Watton PN. Computational fluid dynamics in aneurysm research: critical reflections, future directions. Am J Neuroradiol 2012;33(6):992–5.

[236] Wong GK, Poon W. Current status of computational fluid dynamics for cerebral aneurysms: the clinician's perspective. J Clin Neurosci 2011;18(10):1285–8.
[237] Banerjee RK, Back LH, Back MR, Cho YI. Physiological flow simulation in residual human stenoses after coronary angioplasty. J Biomech Eng 2000;122(4):310–20.
[238] Sazonov I, Yeo SY, Bevan RLT, Xie X, van Loon R, Nithiarasu P. Modelling pipeline for subject-specific arterial blood flow—a review. Int J Numer Methods Biomed Eng 2011;27(12):1868–910.
[239] Zhang J-M, Zhong L, Su B, Wan M, Yap JS, Tham JPL, et al. Perspective on CFD studies of coronary artery disease lesions and hemodynamics: a review. Int J Numer Methods Biomed Eng 2014;30(6):659–80.
[240] Dahl KN, Kalinowski A, Pekkan K. Mechanobiology and the microcirculation: cellular, nuclear and fluid mechanics. Microcirculation (New York, NY) 2010;17(3):179–91.
[241] AlMomani T, Udaykumar HS, Marshall JS, Chandran KB. Micro-scale dynamic simulation of erythrocyte–platelet interaction in blood flow. Ann Biomed Eng 2008;36 (6):905–20.
[242] Bagchi P, Johnson PC, Popel AS. Computational fluid dynamic simulation of aggregation of deformable cells in a shear flow. J Biomech Eng 2005;127(7):1070–80.
[243] Jung J, Lyczkowski RW, Panchal CB, Hassanein A. Multiphase hemodynamic simulation of pulsatile flow in a coronary artery. J Biomech 2006;39(11):2064–73.
[244] Abouali O, Modareszadeh A, Ghaffariyeh A, Tu J. Numerical simulation of the fluid dynamics in vitreous cavity due to saccadic eye movement. Med Eng Phys 2012;34 (6):681–92.
[245] Steck R, Niederer P, Knothe Tate ML. A finite element analysis for the prediction of load-induced fluid flow and mechanochemical transduction in bone. J Theor Biol 2003;220(2):249–59.
[246] Mak AFT, Huang DT, Zhang JD, Tong P. Deformation-induced hierarchical flows and drag forces in bone canaliculi and matrix microporosity. J Biomech 1997;30(1):11–8.
[247] Anderson E, Kaliyamoorthy S, Alexander J, Tate M. Nano-microscale models of perisosteocytic flow show differences in stresses imparted to cell body and processes. Ann Biomed Eng 2005;33(1):52–62.
[248] Anderson EJ, Knothe Tate ML. Idealization of pericellular fluid space geometry and dimension results in a profound underprediction of nano-microscale stresses imparted by fluid drag on osteocytes. J Biomech 2008;41(8):1736–46.
[249] Kamioka H, Kameo Y, Imai Y, Bakker AD, Bacabac RG, Yamada N, et al. Microscale fluid flow analysis in a human osteocyte canaliculus using a realistic high-resolution image-based three-dimensional model. Integr Biol 2012;4(10):1198–206.
[250] Anderson E, Kreuzer S, Small O, Knothe Tate M. Pairing computational and scaled physical models to determine permeability as a measure of cellular communication in micro- and nano-scale pericellular spaces. Microfluid Nanofluid 2008;4 (3):193–204.
[251] Lemaire T, Lemonnier S, Naili S. On the paradoxical determinations of the lacunocanalicular permeability of bone. Biomech Model Mechanobiol 2012;11(7): 933–46.
[252] Lemonnier S, Naili S, Oddou C, Lemaire T. Numerical determination of the lacunocanalicular permeability of bone. Comput Methods Biomech Biomed Eng 2011;14 (sup1):133–5.
[253] Lemaire T, Naïli S, Rémond A. Multiscale analysis of the coupled effects governing the movement of interstitial fluid in cortical bone. Biomech Model Mechanobiol 2006;5 (1):39–52.

[254] Sansalone V, Kaiser J, Naili S, Lemaire T. Interstitial fluid flow within bone canaliculi and electro-chemo-mechanical features of the canalicular milieu. Biomech Model Mechanobiol 2012;12(3):1–21.
[255] Lemaire T, Naïli S, Rémond A. Study of the influence of fibrous pericellular matrix in the cortical interstitial fluid movement with hydroelectrochemical effects. J Biomech Eng 2008;130(1):011001.
[256] Birmingham E, Grogan JA, Niebur GL, McNamara LM, McHugh PE. Computational modelling of the mechanics of trabecular bone and marrow using fluid structure interaction techniques. Ann Biomed Eng 2013;41(4):814–26.
[257] Teo JCM, Teoh SH. Permeability study of vertebral cancellous bone using micro-computational fluid dynamics. Comput Methods Biomech Biomed Eng 2012;15 (4):417–23.
[258] Porter B, Zauel R, Stockman H, Guldberg R, Fyhrie D. 3-D computational modeling of media flow through scaffolds in a perfusion bioreactor. J Biomech 2005;38(3): 543–9.
[259] Huiskes R, Chao E. A survey of finite element analysis in orthopedic biomechanics: the first decade. J Biomech 1983;16(6):385–409.
[260] Prendergast PJ. Finite element models in tissue mechanics and orthopaedic implant design. Clin Biomech 1997;12(6):343–66.
[261] Doblaré M, Garcıa J, Gómez M. Modelling bone tissue fracture and healing: a review. Eng Fract Mech 2004;71(13):1809–40.
[262] Giorgi M, Carriero A, Shefelbine SJ, Nowlan NC. Mechanobiological simulations of prenatal joint morphogenesis. J Biomech 2014;47(5):989–95.
[263] Isaksson H. Recent advances in mechanobiological modeling of bone regeneration. Mech Res Commun 2012;42:22–31.
[264] Müller R, Rüegsegger P. Three-dimensional finite element modelling of non-invasively assessed trabecular bone structures. Med Eng Phys 1995;17(2):126–33.
[265] van Rietbergen B, Weinans H, Huiskes R, Odgaard A. A new method to determine trabecular bone elastic properties and loading using micromechanical finite-element models. J Biomech 1995;28(1):69–81.
[266] Coughlin TR, Niebur GL. Fluid shear stress in trabecular bone marrow due to low-magnitude high-frequency vibration. J Biomech 2012;45(13):2222–9.
[267] Metzger TA, Kreipke TC, Vaughan TJ, McNamara LM, Niebur GL. The in situ mechanics of trabecular bone marrow: the potential for mechanobiological response. J Biomech Eng 2015;137(1):011006–7.
[268] Metzger TA, Niebur GL. Comparison of solid and fluid constitutive models of bone marrow during trabecular bone compression. J Biomech 2016;49(14):3596–601.
[269] Dolan EB, Vaughan TJ, Niebur GL, Casey C, Tallon D, McNamara LM. How bone tissue and cells experience elevated temperatures during orthopaedic cutting: an experimental and computational investigation. J Biomech Eng 2014;136(2):021019.
[270] Rath Bonivtch A, Bonewald LF, Nicolella DP. Tissue strain amplification at the osteocyte lacuna: a microstructural finite element analysis. J Biomech 2007;40 (10):2199–206.
[271] Varga P, Hesse B, Langer M, Schrof S, Männicke N, Suhonen H, et al. Synchrotron X-ray phase nano-tomography-based analysis of the lacunar–canalicular network morphology and its relation to the strains experienced by osteocytes in situ as predicted by case-specific finite element analysis. Biomech Model Mechanobiol 2015;14 (2):267–82.

[272] Verbruggen SW, Vaughan TJ, McNamara LM. Strain amplification in bone mechanobiology: a computational investigation of the in vivo mechanics of osteocytes. J R Soc Interface 2012;9(75):2735–44.
[273] Mullen CA, Vaughan TJ, Voisin MC, Brennan MA, Layrolle P, McNamara LM. Cell morphology and focal adhesion location alters internal cell stress. J R Soc Interface 2014;11(101):20140885.
[274] Mullen Conleth A, Vaughan Ted J, Billiar Kristen L, McNamara Laoise M. The effect of substrate stiffness, thickness, and cross-linking density on osteogenic cell behavior. Biophys J 2015;108(7):1604–12.
[275] Barreto S, Perrault CM, Lacroix D. Structural finite element analysis to explain cell mechanics variability. J Mech Behav Biomed Mater 2014;38:219–31.
[276] Cataloglu A, Clark RE, Gould P. Refined stress analysis of human aortic heart valves. J Eng Mech Div 1976;102(1):135–50.
[277] Cataloglu A, Clark RE, Gould PL. Stress analysis of aortic valve leaflets with smoothed geometrical data. J Biomech 1977;10(3):153–8.
[278] Chong M, Eng M, Missirlis Y. Aortic valve mechanics part II: a stress analysis of the porcine aortic valve leaflets in diastole. Biomater Med Devices Artif Organs 1978;6(3):225–44.
[279] Hamid M, Sabbah HN, Stein PD. Comparison of finite element stress analysis of aortic valve leaflet using either membrane elements or solid elements. Comput Struct 1985;20(6):955–61.
[280] Hamid MS, Sabbah HN, Stein PD. Large-deformation analysis of aortic valve leaflets during diastole. Eng Fract Mech 1985;22(5):773–85.
[281] Grande KJ, Cochran RP, Reinhall PG, Kunzelman KS. Stress variations in the human aortic root and valve: the role of anatomic asymmetry. Ann Biomed Eng 1998;26(4):534–45.
[282] Grande KJ, Cochran RP, Reinhall PG, Kunzelman KS. Mechanisms of aortic valve incompetence in aging: a finite element model. J Heart Valve Dis 1999;8(2):149–56.
[283] Grande-Allen KJ, Cochran RP, Reinhall PG, Kunzelman KS. Finite-element analysis of aortic valve-sparing: influence of graft shape and stiffness. IEEE Trans Biomed Eng 2001;48(6):647–59.
[284] Kunzelman K, Cochran R, Chuong C, Ring W, Verrier ED, Eberhart R. Finite element analysis of the mitral valve. J Heart Valve Dis 1993;2(3):326–40.
[285] Black M, Howard I, Huang X, Patterson E. A three-dimensional analysis of a bioprosthetic heart valve. J Biomech 1991;24(9):793797–5801.
[286] Howard I, Patterson E, Yoxall A. On the opening mechanism of the aortic valve: some observations from simulations. J Med Eng Technol 2003;27(6):259–66.
[287] Sacks MS, Yoganathan AP. Heart valve function: a biomechanical perspective. Philos Trans R Soc Lond B: Biol Sci 2007;362(1484):1369–91.
[288] Lim C, Zhou E, Quek S. Mechanical models for living cells—a review. J Biomech 2006;39(2):195–216.
[289] Mofrad MR, Kamm RD. Cytoskeletal mechanics: models and measurements in cell mechanics. Cambridge, United Kingdom: Cambridge University Press; 2006.
[290] Carter DR, Wong M. Modelling cartilage mechanobiology. Philos Trans R Soc Lond B: Biol Sci 2003;358(1437):1461–71.
[291] Buganza Tepole A, Joseph Ploch C, Wong J, Gosain AK, Kuhl E. Growing skin: a computational model for skin expansion in reconstructive surgery. J Mech Phys Solids 2011;59(10):2177–90.

[292] Socci L, Pennati G, Gervaso F, Vena P. An axisymmetric computational model of skin expansion and growth. Biomech Model Mechanobiol 2007;6(3):177–88.
[293] Zöllner AM, Buganza Tepole A, Kuhl E. On the biomechanics and mechanobiology of growing skin. J Theor Biol 2012;297:166–75.
[294] Zöllner AM, Holland MA, Honda KS, Gosain AK, Kuhl E. Growth on demand: reviewing the mechanobiology of stretched skin. J Mech Behav Biomed Mater 2013;28:495–509.
[295] Li NY, Heris HK, Mongeau L. Current understanding and future directions for vocal fold mechanobiology. J Cytol Mol Biol 2013;1(1):001.
[296] Kelleher JE, Zhang K, Siegmund T, Chan RW. Spatially varying properties of the vocal ligament contribute to its eigenfrequency response. J Mech Behav Biomed Mater 2010;3(8):600–9.
[297] Vaughan TJ, Verbruggen SW, McNamara LM. Are all osteocytes equal? Multiscale modelling of cortical bone to characterise the mechanical stimulation of osteocytes. Int J Numer Methods Biomed Eng 2013;29(12):1361–72.
[298] Vaughan T, Voisin M, Niebur G, McNamara L. Multiscale modeling of trabecular bone marrow: understanding the micromechanical environment of mesenchymal stem cells during osteoporosis. ASME J Biomech Eng 2014;.
[299] Nishii K, Reese G, Moran EC, Sparks JL. Multiscale computational model of fluid flow and matrix deformation in decellularized liver. J Mech Behav Biomed Mater 2016;57:201–14.
[300] Wyczalkowski MA, Chen Z, Filas BA, Varner VD, Taber LA. Computational models for mechanics of morphogenesis. Birth Defects Res C: Embryo Today 2012;96 (2):132–52.
[301] Tang D, Yang C, Geva T, Rathod R, Yamauchi H, Gooty V, et al. A multiphysics modeling approach to develop right ventricle pulmonary valve replacement surgical procedures with a contracting band to improve ventricle ejection fraction. Comput Struct 2013;122(Suppl. C):78–87.
[302] Vaughan TJ, Haugh MG, McNamara LM. A fluid–structure interaction model to characterize bone cell stimulation in parallel-plate flow chamber systems. J R Soc Interface 2013;10(81).
[303] Zhao F, Vaughan T, McNamara L. Multiscale fluid–structure interaction modelling to determine the mechanical stimulation of bone cells in a tissue engineered scaffold. Biomech Model Mechanobiol 2015;14(2):231–43.
[304] Zhao F, Vaughan T, McNamara L. Quantification of fluid shear stress in bone tissue engineering scaffolds with spherical and cubical pore architectures. Biomech Model Mechanobiol 2015;1–17.
[305] Khayyeri H, Barreto S, Lacroix D. Primary cilia mechanics affects cell mechanosensation: a computational study. J Theor Biol 2015;379:38–46.
[306] Verbruggen SW, Vaughan TJ, McNamara LM. Mechanisms of osteocyte stimulation in osteoporosis. J Mech Behav Biomed Mater 2016;62:158–68.
[307] Vaughan TJ, Mullen CA, Verbruggen SW, McNamara LM. Bone cell mechanosensation of fluid flow stimulation: a fluid–structure interaction model characterising the role integrin attachments and primary cilia. Biomech Model Mechanobiol 2015;14 (4):703–18.
[308] Boyle C, Lennon AB, Early M, Kelly D, Lally C, Prendergast P. Computational simulation methodologies for mechanobiological modelling: a cell-centred approach to neointima development in stents. Philos Trans R Soc Lond A: Math Phys Eng Sci 2010;368(1921):2919–35.

[309] Garbey M, Rahman M, Berceli S. A multiscale computational framework to understand vascular adaptation. J Comput Sci 2015;8:32–47.
[310] Hoekstra AG, Alowayyed S, Lorenz E, Melnikova N, Mountrakis L, van Rooij B, et al. Towards the virtual artery: a multiscale model for vascular physiology at the physics–chemistry–biology interface. Philos Trans R Soc A 2016;374(2080): 20160146.
[311] Nolan DR, Lally C. An investigation of damage mechanisms in mechanobiological models of in-stent restenosis. J Comput Sci 2017;24:132–42.
[312] Zahedmanesh H, Lally C. A multiscale mechanobiological modelling framework using agent-based models and finite element analysis: application to vascular tissue engineering. Biomech Model Mechanobiol 2012;11(3):363–77.
[313] Zahedmanesh H, Van Oosterwyck H, Lally C. A multi-scale mechanobiological model of in-stent restenosis: deciphering the role of matrix metalloproteinase and extracellular matrix changes. Comput Meth Biomech Biomed Eng 2014;17(8):813–28.
[314] Caiazzo A, Evans D, Falcone J-L, Hegewald J, Lorenz E, Stahl B, et al. A complex automata approach for in-stent restenosis: two-dimensional multiscale modelling and simulations. J Comput Sci 2011;2(1):9–17.
[315] Marom G. Numerical methods for fluid–structure interaction models of aortic valves. Arch Comput Meth Eng 2015;22(4):595–620.
[316] Keating T, Wolf P, Scarpace F. An improved method of digital image correlation. Photogramm Eng Remote Sens 1975;41(8).
[317] Pan B, Qian K, Xie H, Asundi A. Two-dimensional digital image correlation for in-plane displacement and strain measurement: a review. Meas Sci Technol 2009;20 (6):062001.
[318] Berfield TA, Patel JK, Shimmin RG, Braun PV, Lambros J, Sottos NR. Fluorescent image correlation for nanoscale deformation measurements. Small 2006;2(5):631–5.
[319] Evans SL, Holt CA. Measuring the mechanical properties of human skin in vivo using digital image correlation and finite element modelling. J Strain Anal Eng Des 2009;44 (5):337–45.
[320] Staloff IA, Guan E, Katz S, Rafailovitch M, Sokolov A, Sokolov S. An in vivo study of the mechanical properties of facial skin and influence of aging using digital image speckle correlation. Skin Res Technol 2008;14(2):127–34.
[321] Genovese K, Casaletto L, Humphrey JD, Lu J, editors. Digital image correlation-based point-wise inverse characterization of heterogeneous material properties of gallbladder in vitro. Proc R Soc A 2014;470(2167):20140152.
[322] Genovese K, Lee Y, Lee A, Humphrey J. An improved panoramic digital image correlation method for vascular strain analysis and material characterization. J Mech Behav Biomed Mater 2013;27:132–42.
[323] Zhang D, Eggleton CD, Arola DD. Evaluating the mechanical behavior of arterial tissue using digital image correlation. Exp Mech 2002;42(4):409–16.
[324] Zhou B, Ravindran S, Ferdous J, Kidane A, Sutton MA, Shazly T. Using digital image correlation to characterize local strains on vascular tissue specimens. J Vis Exp 2016; (107):e53625.
[325] Cheng T, Dai C, Gan RZ. Viscoelastic properties of human tympanic membrane. Ann Biomed Eng 2007;35(2):305–14.
[326] Verhulp E, Bv R, Huiskes R. A three-dimensional digital image correlation technique for strain measurements in microstructures. J Biomech 2004;37(9):1313–20.
[327] Krehbiel JD, Lambros J, Viator J, Sottos N. Digital image correlation for improved detection of basal cell carcinoma. Exp Mech 2010;50(6):813–24.

[328] Huang J, Pan X, Peng X, Zhu T, Qin L, Xiong C, et al. High-efficiency cell-substrate displacement acquisition via digital image correlation method using basis functions. Opt Lasers Eng 2010;48(11):1058–66.
[329] Verbruggen SW, Mc Garrigle MJ, Haugh MG, Voisin MC, McNamara LM. Altered mechanical environment of bone cells in an animal model of short- and long-term osteoporosis. Biophys J 2015;108(7):1587–98.
[330] Wan LQ, Ronaldson K, Park M, Taylor G, Zhang Y, Gimble JM, et al. Micropatterned mammalian cells exhibit phenotype-specific left-right asymmetry. Proc Natl Acad Sci U S A 2011;108(30):12295–300.
[331] Ahola A, Kiviaho AL, Larsson K, Honkanen M, Aalto-Setälä K, Hyttinen J. Video image-based analysis of single human induced pluripotent stem cell derived cardiomyocyte beating dynamics using digital image correlation. Biomed Eng Online 2014;13(1):39.
[332] Westerweel J, Elsinga GE, Adrian RJ. Particle image velocimetry for complex and turbulent flows. Annu Rev Fluid Mech 2013;45:409–36.
[333] Adrian RJ. Particle-imaging techniques for experimental fluid mechanics. Annu Rev Fluid Mech 1991;23(1):261–304.
[334] Willert CE, Gharib M. Digital particle image velocimetry. Exp Fluids 1991;10(4):181–93.
[335] Arjunon S, Rathan S, Jo H, Yoganathan AP. Aortic valve: mechanical environment and mechanobiology. Ann Biomed Eng 2013;41(7):1331–46.
[336] Gunning PS, Saikrishnan N, McNamara LM, Yoganathan AP. An in vitro evaluation of the impact of eccentric deployment on transcatheter aortic valve hemodynamics. Ann Biomed Eng 2014;42(6):1195–206.
[337] Kini V, Bachmann C, Fontaine A, Deutsch S, Tarbell JM. Integrating particle image velocimetry and laser doppler velocimetry measurements of the regurgitant flow field past mechanical heart valves. Artif Organs 2001;25(2):136–45.
[338] Saikrishnan N, Yap C-H, Milligan NC, Vasilyev NV, Yoganathan AP. In vitro characterization of bicuspid aortic valve hemodynamics using particle image velocimetry. Ann Biomed Eng 2012;40(8):1760–75.
[339] Campos Marin A, Grossi T, Bianchi E, Dubini G, Lacroix D. 2D μ-particle image velocimetry and computational fluid dynamics study within a 3D porous scaffold. Ann Biomed Eng 2017;45(5):1341–51.
[340] De Boodt S, Truscello S, Özcan SE, Leroy T, Van Oosterwyck H, Berckmans D, et al. Bi-modular flow characterization in tissue engineering scaffolds using computational fluid dynamics and particle imaging velocimetry. Tissue Eng Part C: Methods 2010;16(6):1553–64.
[341] Sucosky P, Osorio DF, Brown JB, Neitzel GP. Fluid mechanics of a spinner-flask bioreactor. Biotechnol Bioeng 2004;85(1):34–46.
[342] Engelmayr GC, Soletti L, Vigmostad SC, Budilarto SG, Federspiel WJ, Chandran KB, et al. A novel flex-stretch-flow bioreactor for the study of engineered heart valve tissue mechanobiology. Ann Biomed Eng 2008;36(5):700–12.
[343] Rui L, Shigeo W, Ken-ichi T, Takami Y. Confocal micro-PIV measurements of three-dimensional profiles of cell suspension flow in a square microchannel. Meas Sci Technol 2006;17(4):797.
[344] Patrick MJ, Chen C-Y, Frakes DH, Dur O, Pekkan K. Cellular-level near-wall unsteadiness of high-hematocrit erythrocyte flow using confocal μPIV. Exp Fluids 2011;50(4):887–904.

[345] Fan Z, Sun Y, Di C, Tay D, Chen W, Deng CX, et al. Acoustic tweezing cytometry for live-cell subcellular modulation of intracellular cytoskeleton contractility. Sci Rep 2013;3:2176.
[346] Okeyo KO, Adachi T, Sunaga J, Hojo M. Actomyosin contractility spatiotemporally regulates actin network dynamics in migrating cells. J Biomech 2009;42(15):2540–8.
[347] Doxzen K, Vedula SRK, Leong MC, Hirata H, Gov NS, Kabla AJ, et al. Guidance of collective cell migration by substrate geometry. Integr Biol 2013;5(8):1026–35.
[348] Zamir EA, Czirók A, Rongish BJ, Little CD. A digital image-based method for computational tissue fate mapping during early avian morphogenesis. Ann Biomed Eng 2005;33(6):854–65.
[349] Serra-Picamal X, Conte V, Vincent R, Anon E, Tambe DT, Bazellieres E, et al. Mechanical waves during tissue expansion. Nat Phys 2012;8(8):628–34.